UPPSALA
UNIVERSITET

Digital Comprehensive Summaries of Uppsala Dissertations from the Faculty of Pharmacy 153

First-pass Intestinal Metabolism of Drugs

Experiences from in vitro, in vivo and simulation studies

HELENA ANNA THÖRN

ACTA
UNIVERSITATIS
UPSALIENSIS
UPPSALA
2012

ISSN 1651-6192
ISBN 978-91-554-8251-0
urn:nbn:se:uu:diva-165514

Dissertation presented at Uppsala University to be publicly examined in B42, BMC, Husargatan 3, Uppsala. Friday, February 24, 2012 at 09:15 for the degree of Doctor of Philosophy (Faculty of Pharmacy). The examination will be conducted in English.

Abstract
Thörn, H. A. 2012. First-pass Intestinal Metabolism of Drugs: Experiences from *in vitro*, *in vivo* and simulation studies. Acta Universitatis Upsaliensis. *Digital Comprehensive Summaries of Uppsala Dissertations from the Faculty of Pharmacy* 153. 66 pp. Uppsala. ISBN 978-91-554-8251-0.

The bioavailability of a drug can be described as the fraction of an orally administered dose that reaches the systemic circulation and is often limited by first-pass metabolism in the gut and the liver. It is important to have knowledge about these processes since the systemic blood drug concentration is tightly connected to the effect of the drug.

The general aim of this project was to quantitatively examine the role of the intestine in relation to the liver in first-pass metabolism of orally administered drugs. The first-pass metabolism of verapamil and raloxifene was investigated in detail with *in vivo*, *in vitro* and simulation studies, using the pig as an experimental model.

The intestine contributed to the same extent as the liver to first-pass metabolism of R/S-verapamil *in vivo* in pigs. The S-isomer of verapamil was found in lower plasma concentrations compared to the R-isomer after oral dosing. The *in vitro* metabolism of verapamil in pig and human liver showed interspecies similarity and indicated equal intrinsic clearance for R- and S-verapamil. Through physiologically based pharmacokinetic modeling the stereoselectivity was explained by a combination of several processes, including enantioselective plasma protein binding, blood-to-plasma partition, and gut and liver tissue distribution. For raloxifene the intestine was the dominating organ in first-pass glucuronidation *in vivo* in pigs. Furthermore, the raloxifene concentration entering the intestine or the dose administered in the gut did not influence the plasma PK of raloxifene and indicated that the intestinal metabolism was not saturable with clinical relevant doses. For both verapamil and raloxifene, a time-dependent hepatic metabolism was noted with major consequences to the pharmacokinetic of the drugs.

This project has pointed out the importance of intestinal metabolism in the overall first-pass extraction of drugs and indicates that intestinal metabolism should be considered and evaluated early in drug development.

Keywords: pharmacokinetics, metabolism, CYP3A4, CYP2C9, CYP2D6, UGT, glucuronidation, physiologically based pharmacokinetic model, modelling

Helena Anna Thörn, Uppsala University, Department of Pharmacy, Box 580, SE-751 23 Uppsala, Sweden.

ISSN 1651-6192
ISBN 978-91-554-8251-0
urn:nbn:se:uu:diva-165514 (http://urn.kb.se/resolve?urn=urn:nbn:se:uu:diva-165514)

Det är bara att öva och öva och sen en dag så kan man det!

Embla 3,5 år

List of Papers

This thesis is based on the following papers, which are referred to in the text by their Roman numerals.

I **Thörn, H.A.,** Hedeland, M., Bondesson, U., Knutson, L., Yasin, M., Dickinson, P., Lennernäs, H. (2009) Different effects of ketoconazole on the stereoselective first-pass metabolism of R/S-verapamil in the intestine and the liver: important for the mechanistic understanding of first-pass drug-drug interaction. *Drug Metabolism and Disposition*, 37(11):2186-2196

II **Thörn, H.A.,** Lundahl, A., Schrickx, J., Dickinson, P.A., Lennernäs, H. (2011) Drug metabolism of CYP3A4, CYP2C9 and CYP2D6 substrates in pigs and humans. *European Journal of Pharmaceutical Sciences*, 43(3): 89-98

III **Thörn, H.A.,** Sjögren, E., Dickinson, P.A, Lennernäs, H.Binding processes determines the stereoselective intestinal and hepatic extraction of verapamil *in vivo*. *Submitted to Molecular Pharmaceutics.*

IV **Thörn, H.A.,** Yasin, M., Dickinson, P.A., Lennernäs, H.Extensive intestinal glucuronidation of raloxifene *in vivo* in pigs and impact for oral drug delivery.*Submitted to Xenobiotica.*

Reprints of paper I and II were made with permission from the respective publisher.

Contents

Abbreviations

ADME	Absorption, distribution, metabolism, and elimination
AUC	Area under the plasma concentration-time curve
BCS	Biopharmaceutics classification system
BDDCS	Biopharmaceutic drug disposition classification system
B/P	Blood-to-plasma ratio
BPD-DS	Biliopancreatic diversion with duodenal switch
C_p/C_b	Plasma to blood ratio
CL	Clearance
CL_b	Blood clearance
CL_H	Hepatic clearance
CL_{int}	Intrinsic clearance
CYP	Cytochrome P450
E_G	Intestinal extraction
E_H	Hepatic extraction
F	Bioavailability
f_{abs}	Fraction absorbed
fu_{gut}	Unbound fraction in the enterocyte
fu_{mic}	Unbound fraction in the microsomes
fu_P	Unbound fraction in the plasma
HPLC	High performance liquid chromatography
i.j.	Intra-jejunal
i.v.	Intravenous
k_{inact}	Inactivation constant
K_m	Michaelis-Menten constant
K_P	Tissue coefficient constant
LC-MS/MS	Liquid chromatography-tandem mass spectrometry
MDCM	Multiple depletion curves method
MRP	Multidrug resistance protein
NADPH	β-nicotinamide adenine dinucleotide phosphate
PBPK	Physiologically based pharmacokinetic
P_{eff}	Intestinal effective permeability
PK	Pharmacokinetic
P-gp	P-glycoprotein
PD	Pharmacodynamic
Q_H	Hepatic blood flow
R-4-G	Raloxifene-4′-β-glucuronide

R-6-G	Raloxifene-6-β-glucuronide
T	Treatment group
$t_{1/2}$	Half life
UGTs	Uridine Diphosphate Glucuronosyltransferases
UV	Ultra-violet
VER	Verapamil
VF	Femoral vein
VH	Hepatic vein
V_{max}	Theoretical maximum metabolic rate
VP	Portal vein

Introduction

The systemic bioavailability (F) of orally administered drugs is often limited by first-pass biotransformation. It is important to have insight into these processes since the effect of the drug is tightly controlled by the systemic blood drug concentration. The liver is a well known site for drug metabolism but during the last two decades enzymes in the intestine has also been recognized as playing a major role in first-pass extraction. The cytochrome P450 (CYP) enzymes and Uridine Diphosphate Glucuronosyltransferases (UGTs) together represent the most important enzymes involved in biotransformation of drugs in humans. Intestinal first-pass extraction (E_G) of CYP3A4 substrates has been extensively investigated and often shown to be high and comparable to the pre-systemic hepatic extraction (E_H) of the drug. The *in vitro* expression and activity of gut wall UGT enzymes have been reported in a number of papers but there is still limited information available on the contribution of intestinal glucuronidation to overall first-pass extraction *in vivo*. This thesis includes studies of two model compounds, R/S-verapamil (R/S-VER) and raloxifene, which are extensively metabolized during first-pass. R/S-VER serves as an example of a substrate that undergoes metabolism by the CYP3A enzyme family and raloxifene is a UGT substrate. The quantitative contribution of the intestine and the liver to first-pass extraction of R/S-VER and raloxifene was investigated *in vitro*, *in vivo*, and *in silico* (with simulation studies), using pig as experimental model.

Bioavailability of a drug

The F of a drug can be described as the fraction of an orally administered dose that reaches the systemic circulation or target site[1]. F is determined by a number of factors and is calculated according to equation 1 (Figure 1).

$$F = f_{abs} (1-E_G) (1-E_H) \quad (1)$$

Before a drug becomes available for absorption, the solid tablet has to disintegrate into smaller particles that are subsequently dissolved in the gastrointestinal fluid into drug molecules. A fraction of the administered dose will be absorbed by the enterocytes (f_{abs}), where the drug molecules might either be effluxed back into the lumen, undergo intestinal metabolism, or transported

to the portal vein (VP). The blood in the VP transfers the drug to the liver before it finally reaches the systemic circulation. In the liver, the drug can undergo hepatic extraction, which includes metabolism and/or excretion into bile. The sum of the extraction that occurs in the intestine and the liver is referred to as the first-pass or pre-systemic extraction, or metabolism of the drug. Since the pharmacological and toxicological effects of most drugs are profoundly influenced by the systemic blood concentration levels of the drug compound, the F is an important determinant of the drug´s efficacy and adverse effects[2]. Alterations in any of the factors that determine the F can affect the blood drug level, and may ultimately lead to loss of the pharmacological effect or to drug-induced toxicity. Such alterations, for example, can occur in a disease state, or as a result of food-drug or drug-drug interactions[3, 4].

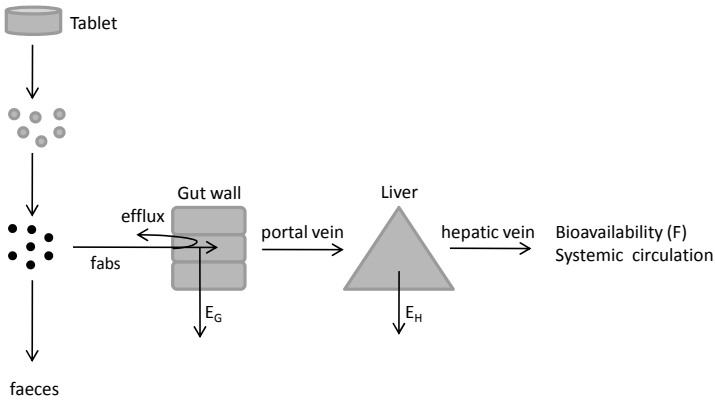

*Figure 1.*The barriers a drug molecule must overcome to reach the systemic circulation and the site of action.

Intestinal absorption and metabolism

Intestinal absorption and metabolism may be controlled by a complex interplay of many factors, including drug lumen concentration, passive permeability, carrier-mediated transport, protein binding, enterocyte blood flow and enzyme activity[5-10]. The anatomy and physiology of the intestine are, along with the physiochemical properties of the drug molecule and the characteristics of the delivery system, central components in determining the extent of absorption from the gut lumen.

Anatomical and physiological considerations

The intestine may be broadly divided into the small and large intestine, which differ in terms of anatomy and function[11-13]. The small intestine plays

the primary role in the digestion and absorption of nutrients and drugs due to its large surface area, which is created by a special anatomical arrangement: the intestinal mucosa is folded and contains the intestinal villi, which are covered by a simple, columnar epithelium that is carpeted with microvilli. This structure increases the total area for absorption by a factor of more than 600. The large intestine is important for the absorption of ions and water but can also play a role in the absorption of drugs, particularly if the dosage form is designed to reach the colon, i.e. modified- or extended-release systems.

The enterocyte

The absorptive cells lining the gut lumen are called enterocytes. These cells are derived from the stem cells located at the base of the villus and differentiate into highly polarized cells during the migration of the stem cells towards the villus tip[11]. The apical membrane of the enterocyte is in contact with the gut lumen while the basolateral membrane faces the blood supply of the tissue. These membranes are formed by tightly fitted cells, separated by tight junctions[14, 15].

The main intestinal absorption mechanism for drugs *in vivo* is considered to be passive, transcellular membrane diffusion with the apical membrane as the rate-limiting step[16, 17].The extent of passive transcellular diffusion depends on the physiochemical properties of the drug, favoring small, lipophilic and non- ionized drug molecules[18, 19].The passive diffusion is driven by the concentration of the drug in the lumen. Apart from passive diffusion, drugs can also be transported through cellular membranes by transporter-mediated influx or efflux (either passive or active), paracellular transport and endocytosis. Passive transcellular and carrier-mediated processes coexist and contribute to drug transport activities across biological membranes[17].

The enterocytes express a broad range of carrier-mediated transporters that may influence the absorption of drugs[20]. Carrier-mediated intestinal absorption of drugs becomes the dominating mechanism for drugs with a reasonable high affinity for any intestinal transport protein, whereas the contribution from passive permeability is small due to the polar nature of the compound[16]. Important efflux transporters expressed in the intestine are P-glycoprotein (P-gp; ABCB1), breast cancer resistance protein (ABCG2),and multidrug resistance protein (MRP) 2 (ABCC2)[20]. P-gp is reported to play an important role in limiting the oral F of many compounds, including cyclosporine[21], digoxin[22], paclitaxel[23], and numerous HIV-1 protease inhibitors[24].

Enzymatic activity in the gut wall

The enterocytes contain a number of enzymes that may limit the total systemic exposure of a drug. The most important enzymes involved in biotransformation of drugs in humans are the CYPs[25]. In addition to the liver, where

the CYPs are predominantly found, the CYPs are also expressed in the mucosa of the small intestine, lung, kidney, brain, olfactory mucosa, and skin[26]. Of these tissues, the intestinal mucosa is probably the most important extrahepatic site of drug biotransformation, since drug molecules must pass through the enterocytes after oral administration. Glucuronidation and sulfation are the most important phase 2 reactions in the biotransformation of drugs[27-29]. The biotransformation enzymes, UGTs and the sulfotransferases, are distributed widely in many tissues, including the intestine[30-32].

Intestinal CYPs

As in the liver, CYP3A is the most abundant CYP subfamily expressed in the small intestine, accounting for 82% of the total intestinal CYP content[33]. Using immunoblotting techniques, the levels of CYP3A4 have been estimated to be 160, 120, and 70 pmol/mg of microsomal protein in the duodenum, jejunum, and ileum, respectively[34]. These values are comparable to the CYP3A4 content in the liver (350 pmol/mg of microsomal protein)[34]. However, the CYP enzymes are expressed only in the enterocytes, which account for only a very small fraction of the total intestinal cell population. In addition, the human liver is about twice as large as the small intestine by weight. This means that, the total mass of CYP3A in the entire small intestine is only approximately 1% of that in the liver[35, 36]. The expression of CYP3A5 in human small intestine follows a polymorphic pattern similar to that found in liver[33].

CYP2C9 represents the second most abundant CYP in the human intestine (15%), followed by CYP2C19 (2.9%), CYP2J2 (1.4%), and CYP2D6 (1%)[33]. Although these enzymes are expressed and are catalytically active in the small intestine, their low specific contents relative to their hepatic counterparts, suggest that they do not contribute significantly to the first-pass metabolism of drugs[33].

The distribution of CYP enzymes is not uniform along the length of the small intestine. Enteric microsomal CYP3A content, as well as associated catalytic activity, is generally highest in the proximal region and then declines towards the distal ileum[34, 35, 37]. Furthermore, the distribution of CYP enzymes is also un-uniform along the villi within a cross-section of mucosa. The columnar absorptive epithelial cells of the villi exhibit the strongest activity, whereas no activity could be detected in the goblet cells or the epithelial cells in the crypts[38]. Also in common with hepatic CYP, there is considerable inter-individual variation in enteric CYP expression[33].

Intestinal UGTs

The human small intestine expresses a range of UGTs, including UGT1A1, UGT1A3, UGT1A4, UGT1A6, UGT1A8, UGT1A10, UGT2B4, UGT2B7, UGT2B10, and UGT2B15[27, 28, 39]. As with the CYPs, but to a lesser extent, the distribution of UGTs is not uniform along the length of the intestine, nor

along the villi within a specific region of the intestine[5]. Gut UGT activity *in vitro* has been reported for estradioland 17β-estradiol[32, 40], ethinyl estradiol[41], acetaminophen[42], p-nitrophenol and bilirubin[43], and morphine[44, 45].Further on, sseveral studies have investigated the relative importance of intestinal and hepatic glucuronidation *in vitro*[46-49]. One study reported that out of nine investigated substrates, two showed an intestinal glucuronidation CL_{int} that was higher than hepatic activity, one with comparable activities for the two organs, and the remaining showed glucuronidation activity that was lower in the intestine compared to the liver[46].

Clinical evidence of intestinal metabolism

A considerable number of *in vivo* studies have demonstrated that the gut mucosa contributes to the overall first-pass metabolism of many drugs. In particular, the E_G of CYP3A substrates is often reported to be high[50-58]. The most direct evidence for a significant contribution of E_G in humans came from studies during the anhepatic phase in patients undergoing liver transplantation, in which drug and metabolite concentrations were determined in VP blood after oral dosing of the parent compound[50, 51, 59]. These studies reported that approximately 50% of the luminal administered amounts of the CYP3A4 substrates felodipine, cyclosporine, and midazolam was metabolized when the drugs reached the VP.

However, ethical and technical limitations in sampling of VP blood in humans has meant that intestinal metabolism in humans has been investigated indirectly by comparing plasma area under the plasma concentration-time curves (AUCs) after intravenous (i.v.) and oral administration. Results using this method suggest that the gut wall mucosa contribute to R/S-VER first-pass metabolism to the same extent as the liver[53, 60].

Using a device for gastrointestinal intubation, that enabled budesonide and concomitant ketoconazole to be administrated at three different locations in the gut (jejunum, ileum and colon), Seidegaard and co-workers could show that CYP3A activity was considerable in the small intestine but absent in the colon[61].

Evidence for a significant contribution of the small intestine in the first-pass metabolism of drugs has also been shown in obese patients that have undergone a bariatric surgery called biliopancreatic diversion with duodenal switch (BPD-DS)[62]. Following a BPD-DS, the entire jejunum is bypassed and it was shown that the F of atorvastatin increased significantly after the-surgery[62]. These results emphasize the protective nature of the proximal small intestine against ingested exogenous compounds. Consequently, re-titration to lowest effective dose should be considered after BPD-DS for drugs with a high degree of intestinal first pass metabolism and a narrow therapeutic window.

In contrast to the extensive investigations of intestinal CYP-activity, few studies have evaluated intestinal drug glucuronidation *in vivo*. Extrahepatic

glucuronidation of propofol was demonstrated in patients during the anhepatic phase of liver transplant operations[63] and while undergoing jugular porto-systemic shunting[64]. However, these studies did not differentiate between renal and intestinal glucuronidation. *In vivo* intestinal conjugation in rats has been reported for phenol, morphine, naloxone, bupronorphine, and napthol[65-68].In conclusion, there is a need for further studies to determine the quantitative contribution of intestinal glucuronidation to drug metabolism.

The drug efflux-metabolism alliance

The considerable overlap in the substrate selectivity and tissue localization of CYP3A and P-gp has led to the hypothesis that this transporter and enzyme pair acts as a coordinated absorption barrier against xenobiotics[69, 70].This hypothesis involves the transporter controlling the access of the drug to the enzyme, giving the enzyme multiple opportunities to prevent the intact xenobiotic from entering the bloodstream (Figure 2)[71]. The E_G of a drug could therefore be changed as a function of P-gp activity without inhibiting or inducing CYP3A enzymes.

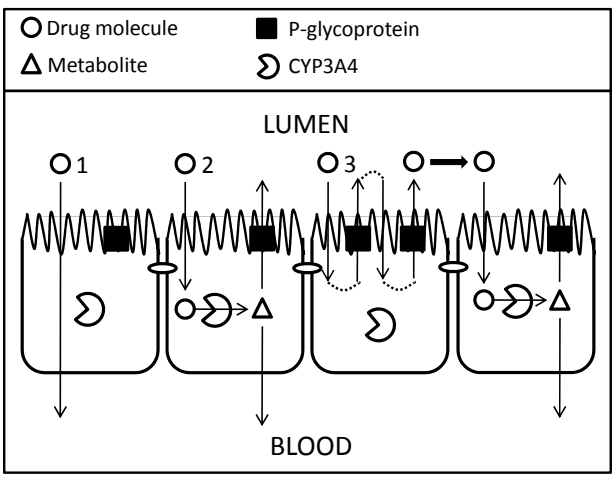

*Figure 2.*The suggested interplay between CYP3A4 and P-gp in the enterocytes working as a coordinately protective mechanism against foreign substances. Three different scenarios are described: 1) A drug molecule is absorbed through the enterocyte by passive transcellular diffusion. The molecule is neither metabolized by CYP3A4, or effluxed by P-glycoprotein. 2) A drug molecule is absorbed by the enterocyte where it is metabolized by CYP3A4. The metabolites are either transported to the blood, or actively effluxed to the lumen. 3) A drug molecule is cycled in and out of the enterocyte by P-gp, giving the enzyme multiple opportunities to prevent the drug molecule from entering the bloodstream.

Hepatic extraction and disposition of drugs

The liver is the most important site for drug elimination in the human body. This is certainly true for drugs given orally since any drug molecule that is absorbed from the gastro-intestinal lumen into the VP must pass through the liver before gaining access to the rest of the body. The process that determines E_H is plasma protein binding, liver blood flow, liver uptake (passive transcellular and carrier-mediated uptake), metabolism and excretion into bile[72, 73].The liver expresses a broad range of enzymes, but the family of CYP enzymes are the most important for the metabolism of drugs[25]. The excretion into bile is a process involving carrier-mediated efflux proteins. Compounds that are excreted into bile reach the intestine and can be either re-absorbed (enterohepatic circulation),or eliminated with feces[74]. It is important to note that enterohepatic cycling is a component of distribution and not elimination.

Hepatic blood flow

The liver receives about 25% of the total cardiac output (total liver blood flow in humans ~1350 ml/min)[75]. Portal blood supplies about two-thirds of the total blood flow to the organ, and arterial blood flow accounts for the remainder. Within the liver, the blood from the VP and hepatic artery merge into the sinusoidal space, which is filled with hepatocytes, and continues to the central veins. The blood leaves the liver and enters the systemic circulation through the hepatic veins (VH).

The hepatocyte

The hepatocytes are polarized cells with three distinct membrane domains: the sinusoidal membrane facing the blood, the canalicular membrane forming the bile canaliculus, and the lateral membrane, which is the connective surface between adjacent pairs of hepatocytes[76]. The hepatocytes are arranged in subunits called the sinusoids and the canalicular and sinusoidal membranes are constituted with microvilli, which enables high exchange of molecules between the perfusing blood and the hepatocytes[76]. Also, membrane transporter proteins are highly expressed on both the canalicular membrane and sinusoidal membrane to facilitate the distribution of endogenous and exogenous entities in and out of the cell[77-79].

Hepatic enzymatic activity

There are a vast number of metabolic enzymes inside the hepatocytes, either integrated with intra-cellular components, such as the endoplasmic reticulum, or freely floating in the cytosol. The family of CYP enzymes are found

in abundance in the human liver[80]. Also other enzymes, such as UGTs, sulfotransferases, and glutathione S-transferases are found in great amounts in the human liver[81]. Humans show large inter-individual variation in the amount of different enzymes, which accounts in part for the large inter-individual variation observed in human drug clearance (CL) and, for some drugs taken per oral, in F. Thus, in some instances, variation in hepatic enzyme expression can contribute to variation in drug response[2].

Hepatic CYPs

In 1994, Shimada and co-workers systematically characterized the specific content of major hepatic CYPs involved in the biotransformation of drugs[82]. The CYP3A subfamily (i.e. CYP3A4 and CYP3A5) was reported as the most abundant, representing 29% of total CYP content. The CYP2C subfamily was the second most abundant (18%), followed by CYP1A2 (13%), CYP2E1 (7%), CYP2A6 (4%), CYP2D6 (<2%), and CYP2B6 (<1%). A considerable large inter-individual variation in the expression of the different CYP isoforms was observed, ranging from 20-fold (CYP2E1 and CYP3A4) to >1000-fold (CYP2D6). Although CYP3A was the major CYP enzyme in the liver and the intestine, its contribution to the intestine was double its contribution to the liver. It is clear that the liver expresses a broader range of enzymes compared to the intestine.

Hepatic UGTs

The liver is the major organ for glucuronidation in the body. Many isoforms of UGT enzymes are expressed in the human liver including: UGT1A1, UGT1A3, UGT1A4, UGT1A6, UGT1A9, UGT2B4, UGT2B7, UGT2B10, UGT2B11, UGT2B15, UGT2B17, and UGT2B28.Glucuronide conjugates have molecular characteristics that are associated with biliary excretion of a compound, i.e. high molecular weight, ionized and presence of polar groups[83]. Hepatic conjugation followed by biliary excretion and intestinal de-conjugation can therefore be part of enterohepatic cycling[74, 81].

Predicting intestinal and hepatic extraction

Early knowledge of properties of absorption, distribution, metabolism, and elimination (ADME) of potential drug candidates is of major importance in the selection processes during drug development, and in reducing cost and time loss related to selection failure[84, 85]. Both empirical and physiologically-based approaches have been developed to predict the *in vivo* intestinal and/or hepatic metabolic CL in animals and humans[86-93]. Traditionally, predictions of human CL have used information from preclinical studies in animals, e.g. allometric scaling, but there has recently been an increase in the use of *in vitro* data and *in vitro* to *in vivo* physiologically-based direct-scaling ap-

proaches[94-97]. The reasons for this development include practical advantages of *in vitro* methods, scientific limitations in the *in vivo* methods, such as species differences, and the possibility of reducing the use of animals[94]. Animal models are still useful, however, when used in conjunction with *in vitro* tools. It is suggested that animal physiologically based pharmacokinetic (PBPK) models should be used as part of a stepwise approach: the first step uses animal to understand the processes and verifies the predictive power of *in vitro* systems, and the second step involves forecasting human pharmacokinetics (PK) from *in vitro* data and *in silico* methods[94].

In vitro to *in vivo* scaling

The first step in predicting drug CL from *in vitro* data is to determine intrinsic CL (CL_{int})[86, 87].*In vitro* CL_{int} values are determined by substrate depletion or metabolite formation in various systems, including hepatocytes, liver or intestinal microsomes, or recombinant CYPs, and normalized for cell, microsomal protein or enzyme concentration. The second step is to determine the *in vivo* CL_{int} by scaling the activity measured *in vitro* to the whole liver, e.g. using a scaling factor that accounts for incomplete microsomal recovery from the tissue. The third, and final step, involves the use of a liver model that incorporates the effects of hepatic blood flow, plasma protein binding and blood cell partitioning to convert the estimated *in vivo* CL_{int} into hepatic CL (CL_H). The well-stirred liver model is most commonly used but the dispersion model or the parallel tube model can also be used.

PBPK models

PBPK models divide the body into anatomically and physiologically meaningful compartments, including the gastrointestinal tract for absorption, the eliminating organs, and non-eliminating tissue compartments[84]. The different compartments are connected to each other by physiologically relevant blood flows. The models use physiological and species-specific parameters (such as tissue volumes and enzyme abundance) to describe the ADME processes. In addition, compound-specific parameters, such as physicochemical and biochemical parameters (e.g. tissue/blood partitioning and metabolic CL) are incorporated into the model. This enables prediction of the profiles of plasma and tissue concentration versus time in an *in vivo* system following i.v. or oral administration of the compound.

PBPK predictions are a valuable tool in the pharmaceutical industry since they facilitate combination of all relevant information generated during the pre-clinical stage[98]. Meaningful data integration helps to improve decision-making during a selection process. In addition, a PBPK model can be used in hypothesis testing and to obtain mechanistic understanding of PK properties

of a drug compound, which is how PBPK modeling was used in the project presented in this thesis.

Several commercially software packages are available that incorporate generic PBPK models for humans or pre-clinical species and PBPK models coupled with PD models[84]. Those models are designed for the pharmaceutical industry and are useful tools for understanding, exploring, predicting, and visualizing PK processes.

Special considerations concerning intestinal modeling

The basic components of the well-stirred liver model (CL_{int} and organ blood flow terms) are also incorporated into intestinal prediction models. However, there are some subtle differences between hepatic and intestinal prediction models[6].

To start with, the blood flow to the mucosa is only a fraction of the total arterial flow to the small intestine. After oral administration, the blood flow is not involved in the delivery of drug to the site of E_G, but it can influence the intracellular residence time-the greater the flow, the lower the E_G.

The unbound fraction of the drug in the enterocyte (fu_{gut}) is another factor that has the potential to influence the extent of E_G. Unfortunately this parameter is difficult to determine experimentally and is usually assumed to be 1[89, 90, 99].

Furthermore, the distribution of drug-metabolizing enzymes is not uniform along the small intestine, or along the villi, and therefore the prediction of drug elimination by the well-stirred model will be less accurate for the small intestine than for the liver. One way of dealing with this problem is to divide the intestine into segments, each defined by a unique pattern of enzyme expression[99-101].

After oral administration, the drug concentration in the enterocytes will be significantly higher than in the hepatocytes. This means that saturable metabolism during drug absorption would be more likely in the intestine than in the liver. Thus, the extent of intestinal first-pass metabolism might be dependent on the oral dose[5].

Verapamil and raloxifene as model compounds

To investigate the relative roles of the intestine and liver in first-pass extraction of drugs, two model compounds were used in the studies included in this thesis: R/S-VER and raloxifene. Both drugs are extensively metabolized in the human body; R/S-VERis metabolized by the CYP system and raloxifene is metabolized by the UGTs.

Verapamil

R/S-VER is a well known nonselective calcium channel blocker with antianginal, antihypertensive, and antiarythmic properties[102, 103].R/S-VER is a basic (pKa 8.66) and lipophilic (log $D_{pH7.4}$ 2.7) compound[104]. Due to its extensive metabolism and high intestinal permeability R/S-VER is classified as a class I drug according to the Biopharmaceutic drug disposition classification system (BDDCS)[105, 106].R/S-VER is also a class I drug according to the Biopharmaceutics classification system (BCS) due to the f_{abs} of more than 90% and as the highest dose is soluble at all three pH´s[52, 107].The commercial brand consists of a racemic mixture of equal amounts of two optical isomers: (+)-(R)-VER and (-)-(S)-VER. The isomers have different PK and PD properties. After oral dosing of the drug, it is well established that the PK is stereoselective, with 5 times higher plasma concentration of the R-isomer[60, 108]. This is despite the similarity in *in vivo* intestinal permeability for the two isomers in humans, pigs and rats[52, 109, 110].After i.v. dosing, however, the stereoselective effect is not as pronounced, with an R- to S-VER plasma ratio of approximately 1.5-2[60, 108].CYP3A4 and CYP3A5 are the predominant isoforms involved in the metabolism of R- and S-VER in humans[111, 112]. Norverapamil and D-617 are the major metabolites formed from R/S-VER(Figure 3).

The reported extensive first-pass metabolism in combination with the high intestinal permeability were the major reasons for choosing R/S-VER as one of the model compounds. Due to its high permeability, the F of a BCS class I drug is insensitive to interactions involving intestinal carrier-mediated transporters. Therefore, we could expect that any changes in AUC or F would be mainly influenced by the extent of metabolism.

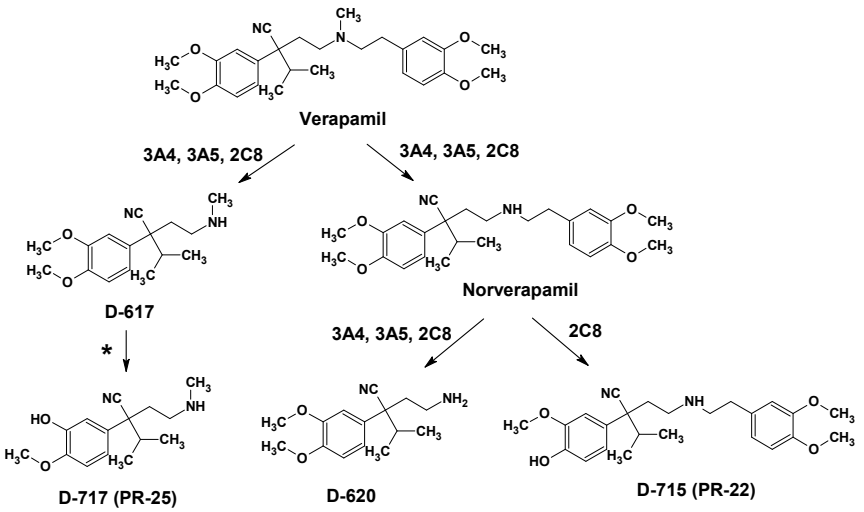

Figure 3. Chemical structure of verapamil and its major metabolites formed through N-dealkylation (D-617) and N-demethylation (norverapamil) and the consecutive biotransformation of the metabolites in humans. The cytochrome CYP enzymes involved in these reactions are specified for each pathway.

Raloxifene

Raloxifene (Evista®) is an orally-administrated, selective estrogen receptor modulator used to treat osteoporosis and prevent breast cancer(Figure 4). The drug belongs to class II according to the BCS and the BDDCS[107, 113]. Raloxifene is a basic (pKa 9.6) and lipophilic compound (logP 5.2) (DrugBank). The PKs of raloxifene are characterized by extensive metabolism, resulting in 2% F. Metabolism of the drug is dominated by glucuronidation, which is responsible for 97 and 50% of the total intestinal and hepatic metabolism, respectively[114]. Raloxifene-4′-β-glucuronide (R-4-G) is the major metabolite but raloxifene-6-β-glucuronide (R-6-G) can also be detected in human plasma. The formation of R-4-G has been shown to be catalyzed primarily by intestinal UGT1A8 and UGT1A10, whereas hepatic UGT1A1 preferentially forms R-6-G[115]. Human jejunum microsomes show high glucuronidation of raloxifene, with a 3-fold greater CL_{int} for R-4-G with jejunal compared to liver microsomes[115]. Despite its low F, raloxifene has a long plasma terminal half-life ($t_{1/2}$) of approximately 27 h, which is attributed to biliary excretion of glucuronide metabolites, de-conjugation in the intestine and enterohepatic recycling[116]. Intestinal efflux mediated by MRP and P-gp has been demonstrated in the Caco-2-cell system[117]. Biliary excretion of raloxifene is reported to be mediated by P-gp[118]. However, the amount of

unchanged raloxifene excreted into bile *in vivo* is presumably low considering the extensive metabolism of the drug.

Raloxifene was chosen as a model compound to demonstrate the glucuronidation capability of the gut wall. From a PK analysis perspective it is advantageous to choose a compound that is directly glucuronidated (instead of consecutive phase II metabolism). Furthermore, high intestinal *in vitro* glucuronidation had already been demonstrated. A BCS and BDDCS class II compound has high permeability and low solubility. However, considering that raloxifene was given as a solution in paper IV it is likely that f_{abs} is close to 1and relatively insensitive to interactions involving intestinal, carrier-mediated transporters.

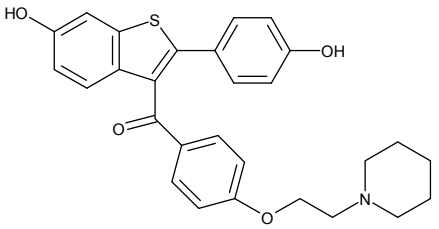

*Figure 4.*The chemical structure of raloxifene

The pig as an experimental animal

The pig is increasingly used as a test animal for both pharmacological and toxicological assessment of new drug compounds. The pig is considered to be appropriate for the investigation of drug disposition, as its physiology is similar to that of the human and the two species have important membrane transport and enzymatic proteins in common[119-121]. The pig in vivo model that our group has developed and validated is ideally suited for predictive mechanistic simulations due to the number of sampling and administration sites available, and the amount of samples that can be taken. Data available on biotransformation in pigs indicates that CYP 1A, CYP2A, and CYP3A enzyme families seem to be very similar between pigs and humans[122-124], while this is not the case for CYP2D and CYP2E[122, 124, 125]. Recently, it was reported that the most abundant CYP subfamilies in pig liver, identified by using MALDI TOF mass spectrometry, were CYP2A, CYP2D, CYP3A and CYP2C[126]. In addition, the CYP enzymes identified showed high primary sequence identity and similarity with the human analogues (80-95% similarity)[126]. Not much is known to date about UGT expression and function in pig intestine and liver.

Aims of the thesis

The general aim of this thesis work was to quantitatively examine the role of the intestine in relation to the liver in first-pass extraction of drugs.

More specifically the aims were:

- To investigate the PK of the CYP3A4 substrate R/S-VER and the UGT-substrate raloxifene in the *in vivo* multisampling site pig model. Special attention was made to obtain a quantitative measurement of E_G and E_H and to organ discrimination of these parameters in the overall first-pass extraction of the drugs.

- To study the effect of local inhibition of gut wall CYP3A enzymes on the PK of intra-jejunally administered R/S-VER in pigs.

- To develop a pig-specific PBPK model suitable for studies of first-pass extraction and evaluate the utility of using the relationship between pre- and post-liver drug concentrations for model discrimination.

- To use the PBPK model to investigate the mechanisms behind the observed stereoselective PK of intra-jejunally administered R/S-VER.

- To characterize the *in vitro* metabolism of four model drugs in pig liver microsomes, and to directly compare the results with corresponding human data.

Methods

The *in vivo* multisampling site pig model

We applied an advanced multisampling site pig model to quantitatively examine the role of intestine in relation to the liver in first-pass extraction of R/S-VER and raloxifene *in vivo*[109, 127-131].It was possible to distinguish between the metabolism that occurred in the gut and the liver by controlled intra-jejunal (i.j.) and i.v. administration and simultaneous venous blood sampling from vessels prior to liver (VP) and subsequent to liver (VH). Blood from the femoral vein (VF) was also collected as a control of the systemic blood concentration.

The *in vivo* studies were performed at the Clinical Research Department, Uppsala University Hospital, Uppsala, Sweden, and were approved by the local ethics committee for the use of laboratory animals in Uppsala, Sweden (C257/6, C 276/9). The pigs included in the studies were of mixed breed (Hampshire, Yorkshire and Swedish landrace), 10-12 weeks old, and had a mean weight of 24±1.3 kg (n=15; VER study) and 25±1.9 kg (n=15; raloxifene study).

The anesthesia and surgical procedure are described in detail in paper I and IV. Briefly, the abdominal cavity was opened with a midline incision and catheters for blood sampling were positioned in the VP, VH and VF veins. Urine and bile was also sampled. A tube for enteral drug administration was inserted into the proximal jejunum. The animals were kept anesthetized, sedated and ventilated throughout the acute experiment. Body temperature, blood gases, electrocardiograms, heart rate, and arterial and central venous pressure were monitored to ensure normal physiological values. At the end of the acute experiment the animals received a lethal dose of potassium chloride while still under anesthesia.

The verapamil study (Paper I)

The R/S-VER study had a parallel group design with four different treatment groups, T1-T4 (Table 1). The pigs in T1 and T2 received racemic R/S-VER dissolved in a solution and single-pass perfused through a 10-cm long intestinal jejunal segment. In T2 a low dose of ketoconazole were administered together with R/S-VER in the perfusion solution. The pigs in T3 and T4 received R/S-VER as a constant infusion into the VP and ear vein, respec-

tively. The experiment lasted for 6 hours and during this time samples were collected from the VP, VH and VF, and from the perfused intestinal segment. Liver and intestinal biopsies, used for mRNA expression analysis (paper II), were collected after the end of the experiment.

Table 1. *The study design in paper I*

Treatment Group	No. of Animals	Drugs	Site of Adm.	Total Dose	Concentration	Rate of Perf./Inf.	Length of Perf./inf.
				mg	mg/ml	ml/h	min
1	4	R/S-VER	J. segm.	240	1.2	120	100
2	4	R/S-VER	J. segm.	240	1.2	120	100
		Keto	J. segm.	8	0.033	120	20+100
3	4	R/S-VER	Portal vein	33	1.0	20	100
4	3	R/S-VER	Ear vein	3	0.5	72	5

Site of Adm., Site of administration; Perf., perfusion; Inf., infusion; J. segm., jejunal segment; Keto, ketoconazole

The raloxifene study (Paper IV)

The study had a parallel group design and consisted of four treatment groups (T1-T4) (Table 2). In the three i.j. groups (T1-T3) raloxifene dose and concentration was varied by varying dose and infusion time to investigate the impact of the total dose given and the lumen concentration on the intestinal glucuronidation of the drug. This is considered to have an impact on the design of the *in vivo* release rate of a drug when developing immediate- and modified-release formulations. The experiment lasted for 6 hours and during this time plasma samples were collected from the VP, VH and VF.

Table 2. *The study design in paper IV*

Treatment Group	No. of Animals	Site of Administration	Total Dose	Concentration	Rate of Infusion	Length of Infusion
			mg	*mg/ml*	*ml/min*	*min*
1	4	Jejunum	60	0.2	10	30
2	4	Jejunum	30	0.2	10	15
3	4	Jejunum	12	0.04	10	30
4	3	S. cava vein	5	0.05	20	5

S.cava vein, superior cava vein

PK analysis

The PK parameters for R/S-VER, ketoconazole and raloxifene were calculated using non-compartmental analysis in WinNonlin 5.2 (Pharsight, Mountain View, CA). The maximal peak plasma concentrations (C_{max}) and the times at which the maximum peaks occurred (t_{max}) were derived directly from each plasma concentration-time profile in all three compartments. The AUC was estimated using the log/linear trapezoidal method. $AUC_{0\text{-}6h}$ was

calculated from time zero to the last measurable concentration point (C_{last}). $AUC_{0-\infty}$ was calculated by extrapolating the curve to infinity by adding $C_{last,extrapolated}/\lambda_z$ to AUC_{0-6h}. λ_z is the first-order elimination rate constant estimated from at least three of the last measurable concentrations after C_{max}. The terminal half life ($t_{1/2}$) was obtained from the elimination rate constant as $\ln 2/\lambda_z$.

Calculations of f_{abs} and P_{eff}

f_{abs} and the intestinal effective permeability (P_{eff}) was calculated in paper I, when R/S-VER was administered via single-pass perfusion of proximal jejunum. The amount that disappeared during the perfusion was assumed to have been absorbed (equation 2).

$$f_{abs} = 1 - ((C_{out} \times PEG_{in}) / (C_{in} \times PEG_{out})) \quad (2)$$

where C_{in} and C_{out} and PEG_{in} and PEG_{out} are the inlet and outlet concentrations of the drug and the non-absorbable volume marker, respectively. Intestinal P_{eff} was calculated according to a well-mixed tank model (equation 3):

$$P_{eff} = ((C_{in} - C_{out}) \times Q_{in}) / (C_{out} \times 2\pi rL) \quad (3)$$

The surface of the cylinder ($2\pi rL$) of the jejunal segment was calculated using the intestinal radius (r=1.25 cm) and the length of the segment (L=10 cm). Q_{in} is the flow rate of the perfusion solution (2 ml/min).

Calculation of intestinal and hepatic extraction

The total plasma CL was calculated by dividing the i.v. dose by the systemically (VF) estimated AUC. Blood CL (CL_b) was obtained by compensating for the plasma to blood ratio (C_p/C_b).

The F was calculated using the dose-corrected $AUC_{0-\infty}$ determined in VF after enteral (PO) or i.v. administration of the drug (equation 4).

$$F = (AUC_{0-\infty,PO} \times Dose_{IV}) / (AUC_{0-\infty,IV} \times Dose_{PO}) \quad (4)$$

Three methods of estimating the E_H were used. One method involved dividing CL_b by the hepatic blood flow (Q_H):

$$E_H = CL_b / Q_H \quad (5)$$

In the second method, AUC_{0-6h} received after administration of R/S-VER in the VP (T3) or in the ear vein (T4) E_H could be estimated without using CL (equation 6).

$$E_H = AUC_{0-6h,T3} / AUC_{0-6h,T4} \quad (6)$$

In the third method, E_H was calculated based on the differences in $AUC_{0\text{-}6h}$ between the VP and VH (equation 7).

$$E_H = (AUC_{0\text{-}6h,VP} - AUC_{0\text{-}6h,VH}) / AUC_{0\text{-}6h,\,VP} \quad (7)$$

Once the estimates of F, f_{abs} and E_H were obtained, the E_G was derived using equation 8:

$$F = f_{abs} \times (1\text{-}E_G) \times (1\text{-}E_H) \quad (8)$$

In the R/S-VER study E_G could also be calculated according to equation 9 by comparing the dose corrected $AUC_{0\text{-}6h}$in VH after i.j. or VP administration of the drug.

$$1\text{-}E_G = (1/f_{abs}) \times (AUC_{0\text{-}6h,i.j.} / AUC_{0\text{-}6h,VP}) \times (Dose_{VP} / Dose_{i.j.}) \quad (9)$$

In vitro investigations

In paper II, the *in vitro* metabolism of R-VER, S-VER, norverapamil, testosterone, diclofenac and dextromethorphan were determined in pig and human liver microsomes. In addition, mRNA expression of the enzymes CYP3A, CYP2C42 and UGT1A1 and of the carrier-mediated transporters ABCB1, ABCC2 and ABCG2 were assessed in small intestinal and liver biopsies from pigs.

Pig and human liver microsomes

Tissues from which liver microsomes could be prepared were taken from male pigs at the local slaughter house in Uppsala, Sweden or at the Clinical Research Department, Uppsala University Hospital, Sweden (ethical approval C257/6). The pigs were of mixed breed (Yorkshire and Swedish landrace) and of the same type as the pigs used in the *in vivo* studies included in this thesis.

Microsomal protein was prepared from pig liver according to classical methods. Briefly, liver tissue were thawed out in cold buffer A(sodium-potassium phosphate buffer, 10 mM, pH 7.4 and 1.14% KCl) and homogenized. The homogenate was centrifuged at 10,000 g for 20 min at 4 °C, and the resulting supernatant was ultracentrifuged at 105, 000 g for 60 min at 4 °C. The pellet was re-suspended with cold buffer A and another ultracentrifugation was performed under the same conditions. The final pellet was re-suspended in buffer B (50 mM potassium phosphate buffer, pH 7.4) and the microsomal protein content was determined using the Lowry method. The

pig liver microsomes were snap-frozen in liquid nitrogen and stored at -80 °C until needed.

Pooled human liver microsomes with a protein content of 20 mg/ml in 250mM sucrose were purchased from BD Gentest (Woburn, MA, USA).

Metabolic assays

Substrate depletion experiments were performed using the so-called multiple depletion curves method (MDCM)[132]. The approach is to generate parent compound depletion curves at multiple concentrations (n=3) and thereafter determine enzyme kinetic parameters by simultaneously fitting the Michaelis-Menten equation to all disappearance curves. Product formation experiments were performed in addition to the depletion experiments for three of the substrates (R-, and S-VER and testosterone) to add more detailed information on one specific metabolic pathway. In general, the microsomal incubations were carried out in triplicate, in a shaking water bath at 37°C. The incubation matrix consisted of KPO_4 buffer (final concentration 0.1 M, pH 7.4) together with pig or human liver microsomes. The reaction was started by the addition of NADPH (final concentration 1 mM) and stopped by transferring the sample to a stop solution (a mixture of organic solvent and internal standard). The concentration of organic solvent did not exceed 0.5 % in the incubations. More specific information about substrate concentration, incubation time, and enzyme protein concentration in the different experiments is given in paper II.

In vitro enzyme kinetic analysis

Data analysis of metabolic assay experiments

The data from the product formation experiments were fitted to the Michaelis-Menten equation (equation 10) using Graph Pad Prim version 4.0 (San Diego, USA).

$$v = (V_{max} \times C)/(K_m + C) \qquad (10)$$

V_{max} is the theoretical maximum metabolic rate and K_m is the Michaelis-Menten constant. K_m describes the substrate concentration (C) at half the V_{max}.

The MDCM was used to analyze the observed substrate depletion data. V_{max} and K_m were estimated by simultaneously fitting the equations to all concentration-time profiles using nonlinear regression in WinNonlin Professional software version 5.2 (Pharsight, Mountain View, CA). The regression was performed with a weighting scheme of $1/([C]^2)$. Two models, one not correcting and one correcting for enzyme-activity-change, were tested for

each dataset and the model giving the lowest coefficient of variation was used to describe the data.

The final parameter V_{max} was normalized to protein concentration and K_m to the unbound fraction in the microsomes (fu_{mic}) before calculating the *in vitro* CL_{int} by dividing V_{max} by K_m.

***In vitro* to *in vivo* scaling**

The *in vitro* CL_{int} for R- and S-VER was used to calculate the *in vivo* CL_{int}according to equation 11:

$$\textit{in vivo}\ CL_{int} = \textit{in vitro}\ CL_{int} \times A_{protein} \times \text{Liver weight} \qquad (11)$$

where $A_{protein}$ is the average recovery of microsomal protein per gram of porcine liver. Using the *in vivo* CL_{int} the CL_H was calculated according to the well-stirred liver model as follows (equation 12):

$$CL_H = Q_H \times fu_P/(B/P) \times \textit{in vivo}\,CL_{int}/(Q_H + fu_P/(B/P) \times \textit{in vivo}\,CL_{int}) \qquad (12)$$

Where fu_P is the unbound fraction of the drug in the plasma and B/P is the blood-to-plasma concentration ratio.

mRNA expression experiments

Liver and intestinal (jejunum) tissues were sampled from eight pigs during the *in vivo* study where the pigs were administered racemic R/S-VER (paper I).Tissue samples were homogenized and total RNA was isolated. Total RNA was quantified spectrophotometrically at 260 nm and first strand cDNA synthesis was performed. Samples were stored at -70°C. Quantitative PCR analysis was performed with primers designed complementary to porcine genes and selected based on efficiency and melting curve analysis.

The mRNA expression levels of the enzymes (CYP3A, CYP2C42, UGT1A1) and transporters (ABCB1, ABCC2, ABCG2) were normalized to the geometric mean expression of the internal control genes glyceraldehyde-3-phosphate dehydrogenase, beta actin and hypoxanthine phosphoribosyltransferase[133]. To compare expression levels between liver and jejunum, the expression levels of biotransformation enzymes and transporters were normalized to the expression of villin.

PBPK modeling

A PBPK model, suitable for PK analysis of data obtained from three plasma sites (VP, VH and VF), after i.j. and i.v. administration of R/S-VER, was constructed using the Berkeley Madonna software. The PBPK model con-

sisted of 8 tissue- and 4 blood-compartments (Figure 5). The compartments were linked together by physiologically relevant blood flows (pig- and human-based) and were given weight (pig-based) and tissue composition (human-based) values that were gathered from the literature[120, 134-136]. A tissue-specific coefficient constant (K_P) was used to determine the tissue distribution at each time point. Initial values of K_P were predicted using the method described by Poulin and Theil[136]. All compartments, except the gut mucosa and liver, were modeled by perfusion-limited distribution. The gut mucosa and liver were modeled as two compartments: a vascular compartment linked to the blood stream, and a cell compartment from which elimination was assumed to occur. An *in vitro* CL_{int} value from the pig model scaled up to an *in vivo* state was used to predict the elimination from the gut mucosa and liver compartments.

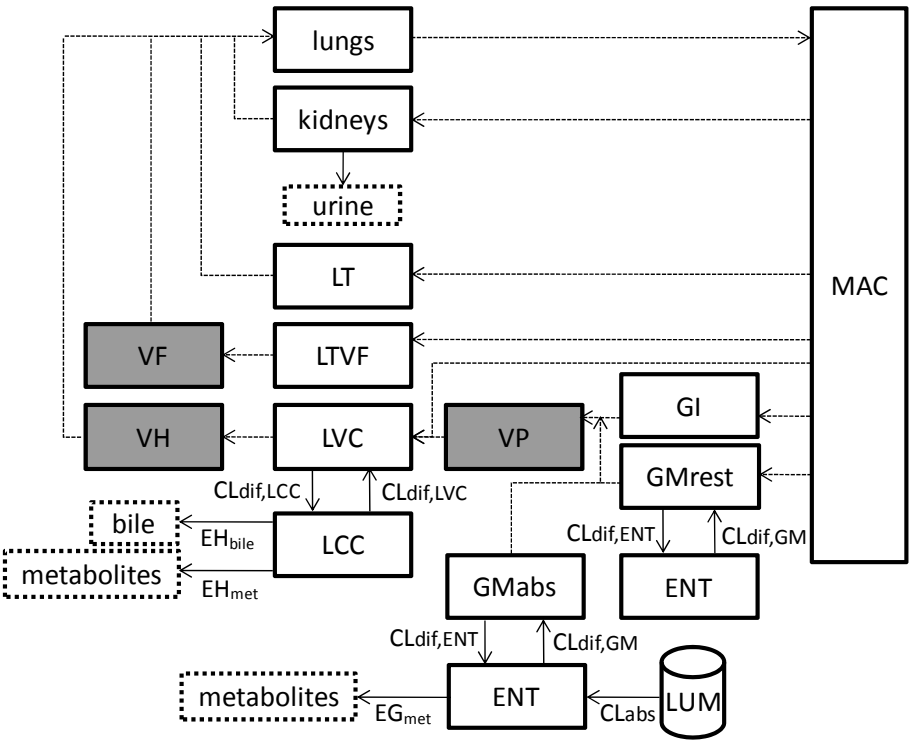

*Figure 5.*The PBPK model. VP, portal vein; VH, hepatic vein; VF, femoral vein; MAC, mixed arterial compartment; GI, gastro-intestinal tract; GMrest, gut mucosa not involved in absorption of drug; GMabs, gut mucosa involved in absorption of drug; ENT, enterocyte; LUM, lumen representing a 10 cm long jejunal segment; LVC, liver vascular compartment; LCC, liver cell compartment; LTVF, lumped tissue associated with VF; LT, lumped tissue

By visual examination and sensitivity analysis the simulated profiles of the VP, VH and VF compartments were optimized to fit the observed plasma concentration-time profiles by allowing changes in parameters affecting the metabolism (CL_{int} gut wall and liver, inactivation constant (k_{inact}) and fu_P) and in the predicted K_P values that were initially introduced in the model. The fit of E_H profile was used for further optimization and discrimination of model parameters. The parameters were first optimized to obtain a fit of the i.v. plasma concentration-time profiles. Optimized clearance and distribution parameters were then applied for the i.j. simulations and only the absorption processes (CL_{int} gut wall, K_P gut mucosa) were adjusted to fit the i.j. plasma profiles. This procedure secured the use of equivalent model settings for both routes of administration.

Bioanalytical methods

None of the papers included in this thesis could have been done without the use of bioanalytical methods to quantify the concentration of the drugs studied and their metabolites. The different methods are described in detail in the respective papers and a summary follows in this section.

Paper I

R-VER, S-VER, R-norverapamil and S-norverapamil were simultaneously quantified using liquid chromatography-tandem mass spectrometry (LC-MS/MS). Trideuterated R/S-VER and norverapamil were used as internal standards. The analytical column was a Chiral AGP and the LC-MS/MS system consisted of an Agilent 1100 liquid chromatography and a Quattro LC quadropole-hexapole-quadropole mass spectrometer.

The ketoconazole concentration in pig plasma was measured by high performance liquid chromatography (HPLC) with electrospray ionization tandem mass spectrometry using econazole as the internal standard. The HPLC system consisted of an Agilent 1100 liquid chromatography and a PE SCIEX API 4000 triple quadrupole mass spectrometer. Separation was performed using a C_{18} Atlantis HPLC column.

Total radioactivity of [^{14}C]-PEG 4000 in the perfusion solution and the perfusate samples was determined by liquid scintillation counting.

Paper II

In paper II, all chemical bioanalysis was performed by HPLC using a Waters 717 HPLC system plus Autosampler and a LC-10AD pump. Ultra-violet (UV) detection was performed using a Spectra 100 UV detector, and fluorometric detection using a FP-1520 Intelligent Fluorescence Detector.

R-VER, S-VER and norverapamil and the internal standards methoxy-VER or diclofenac were isocratically separated on a Hypersil Gold C_{18} column and detected with fluorescence.

Testosterone, the metabolites androstenedione and 6β-OH-testosterone and the internal standard propranolol were separated on a Hypersil Gold C_{18} column. The analytes were detected using UV-detection.

For analysis of diclofenac concentration separation was performed using a Hypersil Gold C_{18} column and detection using UV-detection.

Dextromethorphan was measured by separation on a Reprosil 100 Phenyl column followed by fluorescent detection.

Paper IV

Concentrations of raloxifene and its metabolite R-4-G in pig plasma were measured, after their extraction, by HPLC with electrospray ionization tandem mass spectrometry using a structurally analogous compound as the internal standard. An HPLC system (Agilent Series 1100; Agilent Technologies), equipped with a HTC PAL autoinjector (LEAP Technologies, Carrboro, NC) was used together with a 3.5 µm C18 Atlantis HPLC column (50 x 4.6 mm i.d.; Waters Ltd., Elstree, Herts, UK).

Statistical analysis

For the PK statistical analysis, AUC and C_{max} were assumed to be log-normally distributed and $t_{1/2}$was assumed to be normally distributed. T_{max} was assumed to be a non-parametric parameter and presented as a median and range. Differences were evaluated by a Student's two-sample equal variance (homoscedastic) or paired t-Test, with a two-tailed distribution. Differences between mean values were considered significant at $p < 0.05$.

Results and discussion

Verapamil

R/S-VER was the most extensively studied model compound throughout this project. The results that follow in this section are a summary of the findings obtained from the *in vivo*, *in vitro* and simulation studies included in Paper I-III.

In vivo PK of verapamil in pigs

The PK of R/S-VER was stereoselective in pigs, with higher concentrations of the R-isomer (Figure 6). Comparing the $AUC_{0\text{-}6h}$ of the two enantiomers in the different plasma sampling sites, the difference in concentration was most pronounced in the VH (ratio R/S 2.2) followed by the VF (ratio R/S 1.9) and VP (ratio R/S 1.4). This indicated that the stereoselectivity in peripheral plasma PK occurred mainly during passage through the liver.

The values of F of R/S-VER after i.j. single-pass perfusion were 2.5 and 1.3% for R- and S-VER, respectively (Table 3). The alternative methods for calculating E_H resulted in similar values, around 50%. For E_G, equation 9 gave slightly lower values than equation 8 but the difference was not significant.

Table 3. *First-pass extraction parameters of R- and S-VER after 100 min single-pass perfusion into a 10 cm long jejunal segment. Values are presented as mean ± S.D.*

Parameter	R-VER	S-VER	Equation
F (%)	2.5±1.2	1.3±0.61	4: $F = f_{abs} \times (1\text{-}E_G) \times (1\text{-}E_H)$
f_{abs} (%)	19±9	21±15	2: $f_{abs} = 1 - ((C_{out} \times PEG_{in}) / (C_{in} \times PEG_{out}))$
E_H (%)	50±9	61±6	5: $E_H = CL_H / Q_H$
E_H (%)	48±34	61±34	6: $E_H = AUC_{0\text{-}6h,T3} / AUC_{0\text{-}6h,T4}$
E_H (%)	49±21	68±13	7: $E_H = AUC_{VP} - AUC_{VH} / AUC_{VP}$
E_G (%)	77±4	86±2	8: $E_G = 1 - (F / (f_{abs} \times (1\text{-}E_H{}^a)))$
E_G (%)	61±17	74±13	9: $E_G=(1/f_{abs})\times(AUC_{0\text{-}6h,PO}/AUC_{0\text{-}6h,PV})\times(Dose_{PV}/ Dose_{PO})$

[a]based on E_H from equation 5

Similar to the findings for R/S-VER, the R-isomer of the metabolite norverapamil was found in higher concentrations in plasma than the S-isomer (Figure 6). This is probably due to a higher circulating concentration of R-VER, which enables more R-metabolite to be formed. However, a higher $AUC_{0\text{-}6h}$ R/S ratio of norverapamil compared to R/S-VER also indicated that the consecutive metabolism of the metabolite was stereoselective, with higher loss of the S-isomer.

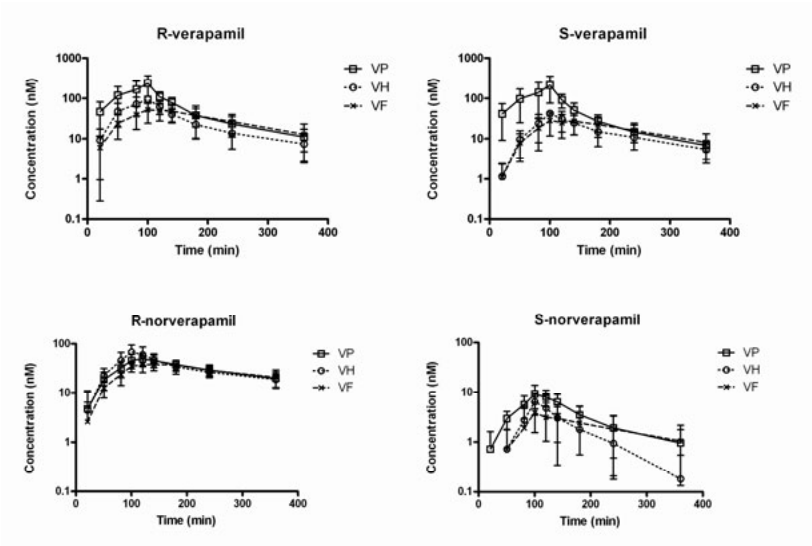

*Figure 6.*The mean ± S.D. plasma concentration-time profiles of R- and S-VERand R- and S-norverapamil in the VP, VH and VF following a 100 min i.j.perfusion of R/S-VER.

After i.v. administration of R/S-VER into the ear vein, R- and S-VER was found in comparable concentrations at the three plasma sampling sites (Figure 7). For norverapamil, only the R-isomer was detectable. The absence of stereoselectivity after i.v. dosing indicates that the first-pass effect is an important factor in determining the difference in isomer plasma concentration after oral administration.

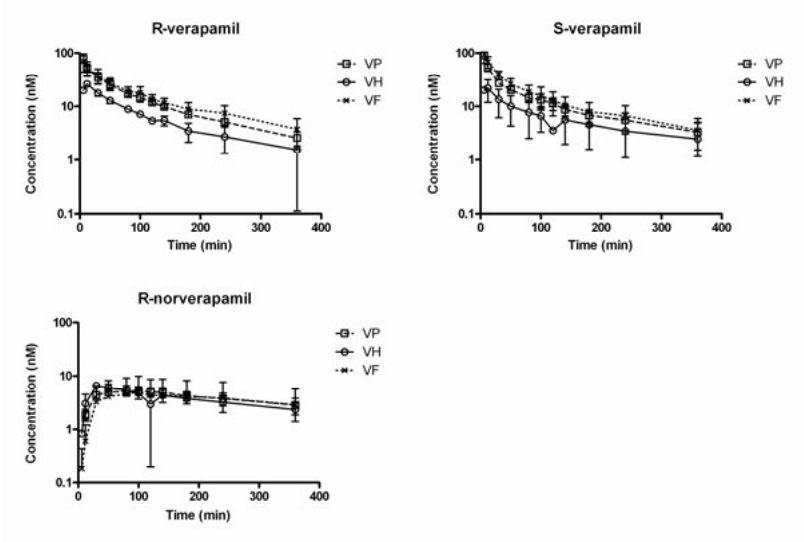

Figure 7. The mean ± S.D. plasma concentration-time profiles of R- and S-VER and R-norverapamil after a 5 min constant infusion of R/S-VER into the ear vein. S-norverapamil was not found in levels above lower limit of quantification.

Pigs versus humans

The PK of R/S-VER in pigs is similar to that of humans (Table 4). Even though the extent of stereoselectivity differs between pigs and humans, it was clear that the PK of R- and S-VER followed the same pattern in both species. In pigs as well as in humans, the S-isomer was found in lower plasma concentrations compared to the R-isomer and the stereoselectivity was more pronounced after i.j. compared to i.v. dosing. Furthermore, the elimination of the drug was comparable between the species, with similar values (no significant difference) of F, CL, $t_{1/2}$, E_G and E_H. However, f_{abs} and P_{eff} was lower in pigs. In general, the P_{eff} values obtained in the pig model were lower than P_{eff} values reported in humans[109, 128].These differences could be explained by anatomical and physiological species differences as well as the surgery/anesthesia used in the pig model.

Table4.*PK parameters of R- and S-VER after i.v. or i.j. administration of R/S-VER in pigs(n=4) and humans (n=6). The values are presented as mean±SD.*

Parameter[a]	**R-verapamil**		**S-verapamil**	
	Pigs	Humans[b]	Pigs	Humans[b]
Dose i.v. (mg)	120	24	120	24
Dose i.j. (mg)	1.5	2.5	1.5	2.5
F (%)[c]	11±6	18±8	6±3	5.3±4.6
f_{abs} (%)	19±9	61±9	21±15	62±9
P_{eff} (10^{-4} cm s^{-1})	0.97±0.50	5.6±2.0	1.15±0.98	5.6±2.0
CL (ml/min)	691±156	588±133	688±104	847±175
C_p/C_b	0.9	1.6	1.1	1.4
CL_b (ml/min)	621±140	938±210	757±115	1190±238
$t_{1/2}$ i.v. (min)	132±49	178±21	138±33	206±26
$t_{1/2}$ i.j. (min)	108±38	174±19	114±16	216±31
E_H (%)	50±9	63±14	61±6	79±16
E_G (%)	77±4	49±18	86±2	68±19

[a]Allcalculations are based on systemic concentrations (VF concentrations in pigs) to allow interspecies comparisons
[b]The human data are obtained from Sandström et al., 1999[60]
[c]TheF is compensated for the loss of drug during the intestinal perfusion

In vitro metabolism of verapamil in pigs and humans

In paper II, the metabolism of both isomers of R/S-VER and the metabolite norverapamil was investigated in pig liver microsomes and directly compared with corresponding human data (Table 5). In pigs, the CL_{int} turned out to be higher for the R-isomer, when measuring both the formation of norverapamil and total loss of parent compound. In human liver microsomes, the values for CL_{int} for R- and S-VER depletion were the same value. We concluded that the lower plasma concentration of S-VER *in vivo* is not likely due to differences in metabolic capacity of the enzymes involved in the biotransformation of R/S-VER. However, the values for *in vitro* CL_{int} were scaled to *in vivo* hepatic CLs using the well-stirred liver model, which indicated that enantiomer differences in fu_P and also the B/P ratio could, to some extent, explain the stereoselectivity of R/S-VER *in vivo*.

Overall, the metabolism of R/S-VER and norverapamil showed higher *in vitro* CL_{int} values in pig-liver microsomes compared to those from the human. Norverapamil was found to be the major metabolite formed from both R- and S-VER in pigs since the CL_{int} determined from formation of norverapamil contributed to 80 and 55% of the depletion CL_{int} value for R- and S-VER, respectively.

Table 5.*Enzyme kinetic parameters describing the metabolism of VER and norverapamil (NOR) in pig (PLM) and human liver microsomes (HLM).*

Substrates	fu_{mic}	V_{max} (pmol/min/mg)	K_m (µM)	CL_{int} (µl/min/mg)
PLM				
Formation of NOR from:				
R-VER	0.51±0.22	1557±46	5.4±0.8	290±11
S-VER	0.56±0.08	2008±70**	17±2.3	116±3.6***
Depletion of:				
R-VER	0.51±0.22	1991±417	5.5±1.3	363±19
S-VER	0.56±0.08	2229±781	11±4.2	210±20
NOR	0.91±0.23	2139±391	3.9±0.7	551±60
HLM				
Depletion of:				
R-VER	0.76±0.11	1101±350	12±4.3	93±7.4
S-VER	0.77±0.66	1257±322	13±3.7	94±13
NOR	0.74±0.07	1733±3830	217±533	8.0±2.3

Values are presented as mean±SD
*·**·***significantly different from R-VER (*p<0.05, **p<0.01, ***p<0.001)

The mechanisms behind the stereoselectivity of verapamil

The plasma concentration time profiles in the VP, VH and VF of R- and S-VER after i.v. and i.j. administration in pigs were successfully captured by the PBPK model (Figure 8). A combination of several processes explained the observed difference in isomer concentration after i.j. administration of R/S-VER in pigs. These differences included enantioselective fu_P, B/P ratio andgut mucosa and liver tissue distribution. The first-pass effect in the gut and the liver after i.j. administration amplified the difference in isomer concentration and explained the absence of stereoselectivity after an i.v. dose. The stereoselectivity of PK was simulated with identical CL_{int} values for R- and S-VER but the higher fu_P and lower B/P for the S-isomer enabled a higher E_H of S-VER.

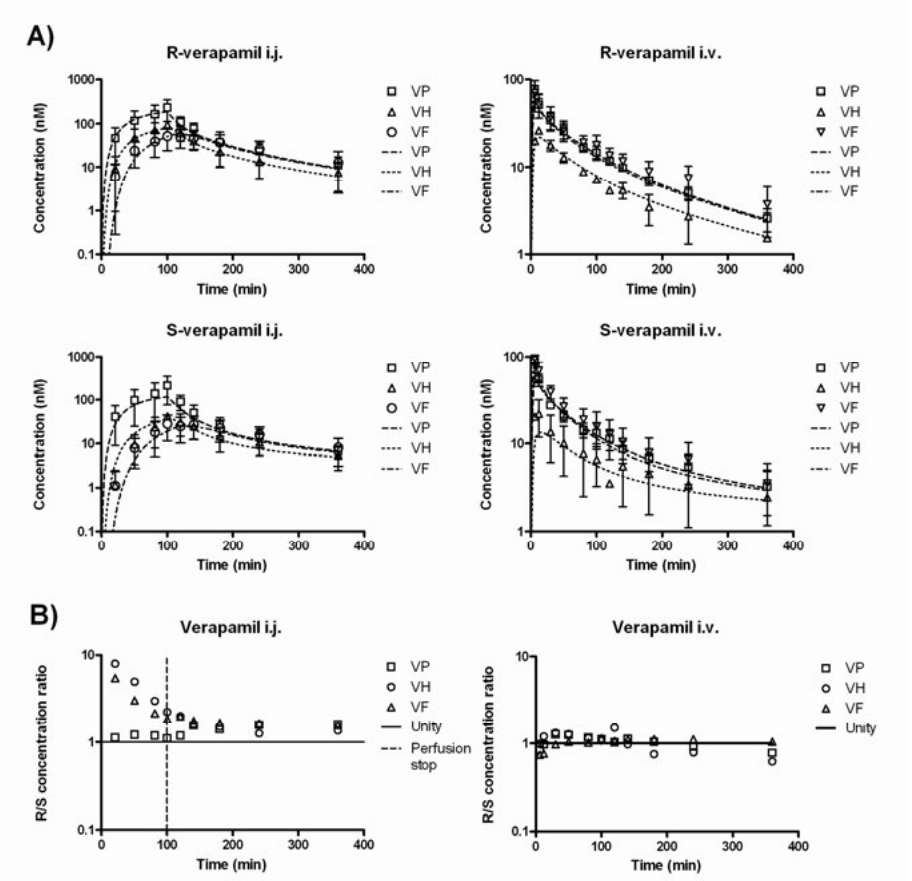

*Figure 8.*A) Observed mean ± S.D. (symbols) and simulated (lines) plasma concentration-time profiles in the VP, VH and VF of R- and S-VER following i.j. or i.v. administration. B) Visualize the observed difference in enantiomer plasma concentration after i.j. administration and the absence of stereoselectivity after i.v. dosing.

The effect of ketoconazole on the PK of verapamil

In the pig *in vivo* study (Paper I), one treatment group received a low dose (8 mg) of ketoconazole together with R/S-VER in the perfusion solution. The purpose of the low dose was to inhibit CYP3A locally in the gut. As expected, the $AUC_{0\text{-}6h}$ in the VP was significantly increased (3.3 ± 1.3-fold and 4.3 ± 2.4-fold for R- and S-VER, respectively; Figure 9). The increase was most likely explained by inhibition of CYP3A-mediated metabolism in the enterocyte, since no significant increase in f_{abs} could be found.

$AUC_{0\text{-}6h}$ increased in the other two plasma sites as well, but the AUC ratio between the control and ketoconazole group was smaller than in the VP. A drug must pass sequentially from the intestinal lumen through the gut wall and liver. Based on this sequence, it was suprising to find that the AUC in-

crease in the VP was not transferred along to the VH, but in fact decreased in the VH. This suggested that the hepatic metabolism was increased in the ketoconazole treatment group but involvement of ketoconazole itself could be excluded since the systemic concentration of this drug was very low. Instead, the 3- to 4-fold increase in R/S-VER and 2- to 2.5-fold increase in norverapamil concentration seen in the VP in the ketoconazole group could have increased the unbound fraction of R/S-VER and thereby increase the amount of drug available for hepatic metabolism.

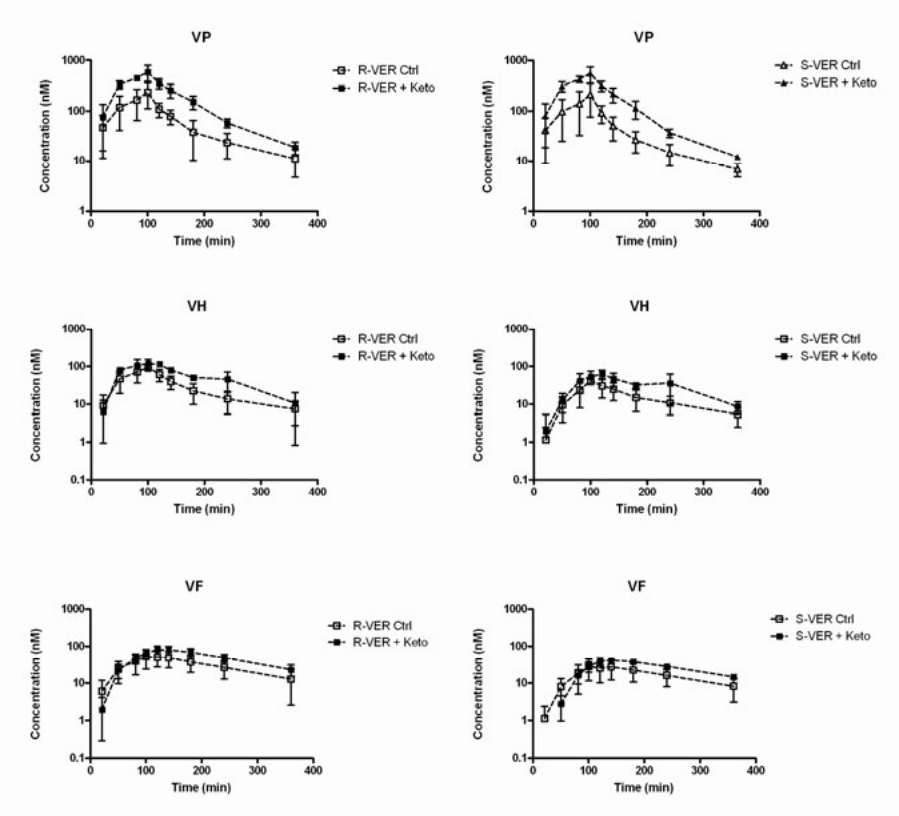

*Figure 9.*Mean ± S.D. plasma concentration-time profiles of R- and S-VER after a 100 min i.j. perfusion of R/S-VER alone (Ctrl) or in combination with ketoconazole (+Keto).

In paper III, the effect of ketoconazole on the PK of R/S-VER was further investigated, including the mechanism involved, by using the pig PBPK model (Figure 10). The increase in R/S-VER VP concentration could be explained mainly by total loss of E_G. In addition to the loss of E_G, the partition of S-VER to the gut mucosa compartment decreased 1.3 times to cover the effect of ketoconazole on the plasma concentration-time profiles of R/S-

VER. Presumably, R/S-VER was partly displaced from the binding sites in the gut mucosa compartment by ketoconazole.

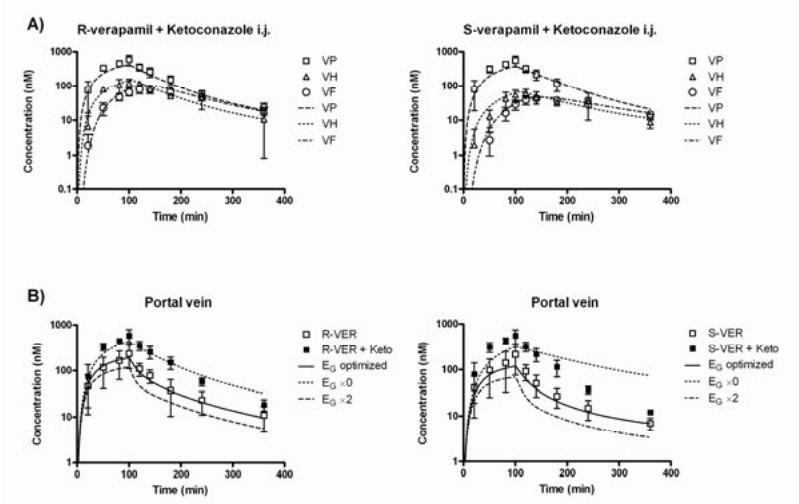

*Figure 10.*A) Observed mean ± S.D. (symbols) and simulated (lines) plasma concentration-time profiles of R- and S-VER with co-administrated of ketoconazole.B) The impact of E_G on the VP concentration of R- and S-VER.

The unexpected increase in E_H in the ketoconazole treatment group was also investigated using the PBPK model and the increase in fu_P hypothesized earlier could indeed cause this effect. A summary of the changes made on the parameters in the control group to simulate the R/S-VER + ketoconazole PK profiles are presented in Table 6.

Table 6. *Changes made on the parameters in the control group to simulate the verapamil + ketoconazole PK profiles.*

Parameter	R-VER+Keto	Change	S-VER+Keto	Change
fuP	0.17 (0.13)	↑1.3	0.51 (0.23)	↑2.2
$CL_{int,G}$ (ml/min/mg)	0 (0.65)	total loss	0 (0.65)	total loss
$K_{P,GM}$	300 (300)	↔	400 (600)	↓1.3

Clearance intrinsic gut ($CL_{int,G}$), tissue partition coefficient gut mucosa ($K_{P,GM}$), ketoconazole (Keto). Values in brackets indicate the parameter values in the control group.

Another observation from the pig *in vivo* study was increased concentration of the metabolite norverapamil in the ketoconazole group compared to control. This could be explained by a higher circulating concentration of R/S-VER in the ketoconazole group, which enables more metabolites to be formed (Figure 11).

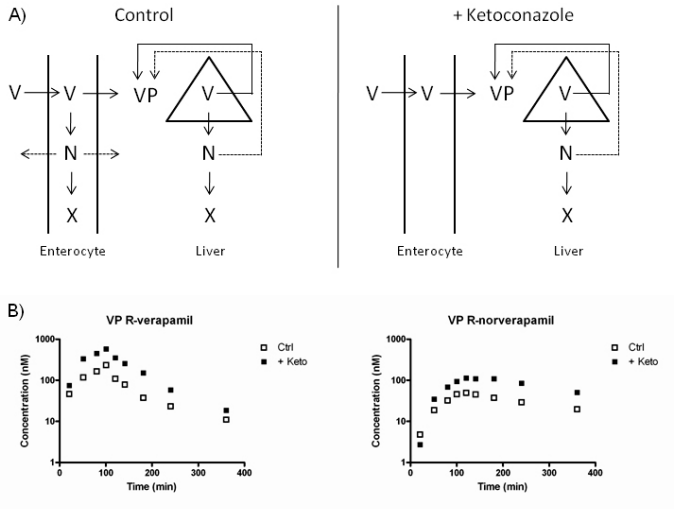

*Figure 11.*A) A schematic picture of the first-pass metabolism of verapamil (V) to norverapamil (N) in the enterocyte and liver following i.j. administration of verapamil alone (control) or together with ketoconazole (+ Ketoconazole). B) The VP concentration of R-norverapamil was increased in the ketoconazole group and is most likely explained by a higher circulating concentration of R-verapamil which enables more metabolite to be formed.

Hepatic expression of CYP3A mRNA versus E_H of VER

In the pig *in vivo* study of R/S-VER, intestinal and liver tissues were sampled at the end of the experiment. The mRNA expression levels of several enzymes and transporters were determined (see section "Pig as experimental animal"). Interestingly, a linear relationship was found between the in vivo E_H, for R-VER, S-VER and the racemate, and liver CYP3A mRNA expression (R^2 = 0.81, 0.75 and 0.84; p=0.015, 0.026 and 0.012 for R-VER, S-VER and the racemate, respectively; Figure 12). This suggests that CYP3A is one of the major enzymes involved in the E_H of R/S-VER in pigs. The plasma PK of other CYP3A4 substrates has also been shown to vary extensively in pigs[129, 137]and the correlation in Figure 12 demonstrates that the level of CYP3A could be a determinant of E_H and plasma PKs of CYP3A substrates in pigs.

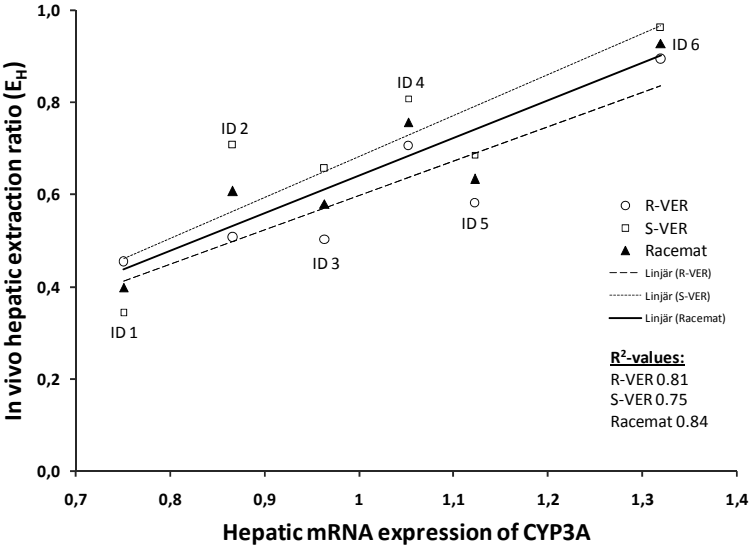

*Figure 12.*A correlation between the *in vivo* E_H of R and S-VER and the hepatic mRNA expression of CYP3A in pigs. Six pigs (ID 1-6) received R/S-VER and E_H was determined by comparing the amount of drug entering and leaving the liver. CYP3A mRNA levels were measured in liver tissue from the same animals.

Time-dependent hepatic extraction

An interesting phenomenon that was noted was a time-dependency in the E_H for R/S-VER. The extraction was high in the beginning but decreased continuously with time (Figure 13). The time-dependency was well described by the PBPK model when k_{inact} was included. The R/S-VER enantiomers and their major metabolites (norverapamil and D-617) are suggested to inhibit CYP3A in a time- and concentration-dependent manner (mechanism-based inhibition)[138-141]. Partition to the liver was important to describe the time-dependency in E_H and had to be relatively high for a good fit (Figure 13D). In general, the E_H is reported as a constant based on AUC calculations. This study demonstrates that a report of such constant E_H value might be a simplified way of describing the liver extraction of drugs during the absorption phase. For R/S-VER, the time-dependent E_H, with high initial extraction, enhances the importance of the oral first-pass effect and further explains the route-dependent stereoselective PK.

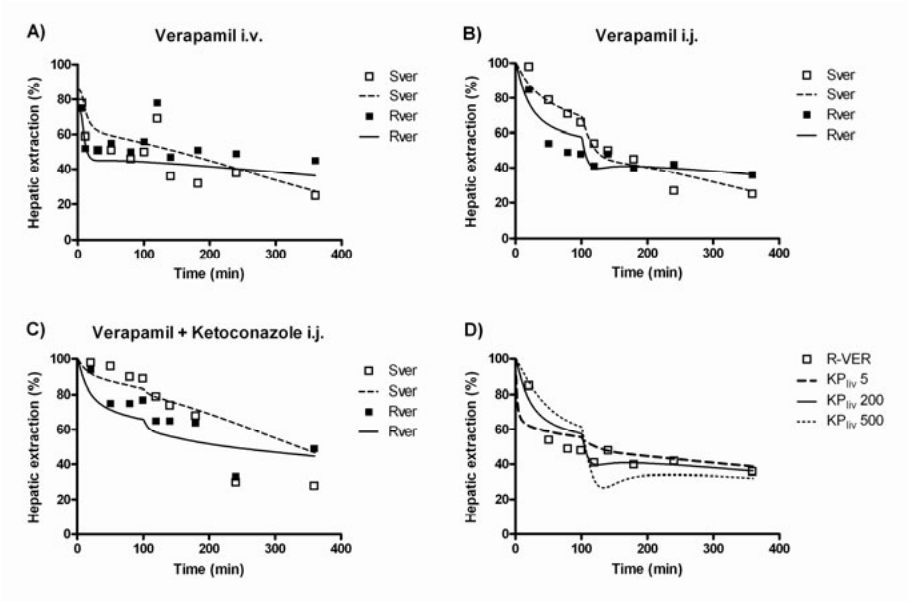

Figure 13. Time-dependent E_H of R- and S-VER after A) i.v. administration,B) i.j. administration, C) i.j. administration together with ketoconazole and D) the impact of tissue partition to the liver (KP_{liv}) on E_H. Squares represent the observed data while lines are the simulated profiles obtained from the PBPK model.

Raloxifene

The first-pass extraction of raloxifene in pigs

Raloxifene was extensively metabolised during first-pass in pigs as evident by values for F of 7.1±3.1 and 6.6±2.6% in T1 and T2, respectively. The extensive metabolism meant that for the low dose treatment group (T3) plasma concentrations were below the lower limit of quantification and so PK parameters could not be calculated. E_G was found to be a major factor determining the low F of raloxifene as the E_G was 85±9.7 and 83±11% in T1 and T2, respectively. The mean E_H of raloxifene was calculated from $AUC_{0\text{-}6h}$ in the portal and VH and was 48±12% in T1 and 53±13% in T2.The intestine is the major organ that forms the 4´-glucuronide metabolite as the intestinal tissue is exposed to a significantly higher concentration of raloxifene during absorption (0.2 mg/ml; 392 µM in T1 and T2) than the raloxifene concentration entering the liver (C_{max} VP: ~0.05 and 0.02 µM in T1 and T2, respectively) (Figure 14).

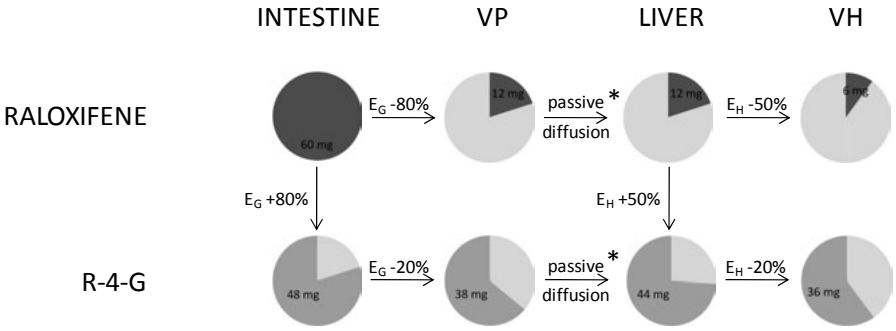

*Figure 14.*A schematic depiction of the contribution of the intestine and liver in extraction of raloxifene in pigs. *Passive diffusion is assumed as the major uptake transport mechanism in the liver

Plasma PK of the metabolite R-4-G

Following i.j. administration of raloxifene, the metabolite R-4-G was found in high concentrations in all plasma sampling sites (Figure 15). However, among the three sites, the highest $AUC_{0\text{-}6h}$ was measured in the VP, resulting in overall hepatic extraction for the metabolite ($E_{H,met}$) of 19±3.5%, 23±5.8% and 40±1.1% in T1, T2 and T3, respectively.

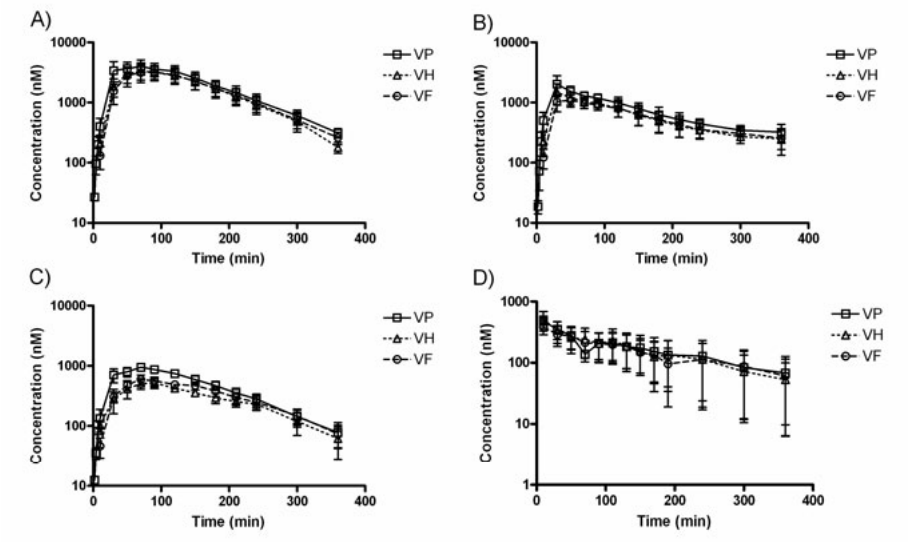

*Figure 15.*Mean plasma concentrations ± S.E. of the metabolite R-4-G in the four parallel treatment groups of pigs.**A)** T1: 60 mg raloxifene i.j. (n=4) **B)** T2: 30 mg raloxifene i.j. (n=4) **C)** T3: 12 mg raloxifene i.j. (n=4) **D)**T4: 5 mg raloxifene i.v. (n=3).

Time-dependent E_H of raloxifene and R-4-G

A time-dependency in E_H was noticed for raloxifene after i.j. administration (Figure 16).Over the time-period studied, the $E_{H,met}$ followed a similar time-dependent pattern as for the E_H of raloxifene. The time-dependency in E_H and the fact that it followed the same pattern for raloxifene and the metabolite suggests that E_H of raloxifene in pigs was affected by the concentration of the metabolite formed, i.e. the metabolite acted as a competitive inhibitor, thus affecting the E_H of raloxifene. There was no time-dependency in E_H following i.v. administration.

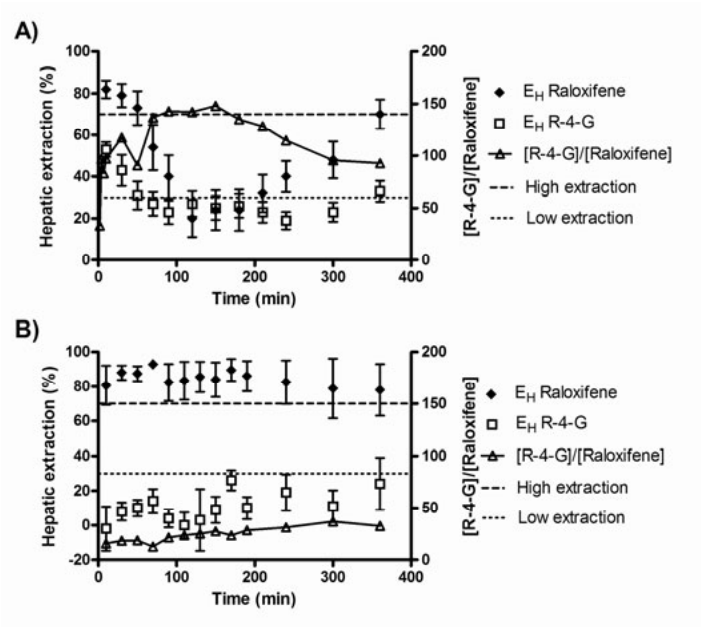

*Figure 16.*The E_H of raloxifene and the metabolite R-4-G over time after **A)**i.j. administration (T1 and T2 together; n=8) and **B)** i.v. administration (T4; n=3). The concentration ratio of R-4-G versus raloxifene ([R-4-G]/[Raloxifene]) is displayed to illustrate the potential of the metabolite as an inhibitor of the E_H of raloxifene. The values are displayed as mean±S.E.M.

E_G and impact of dosage form

The aim of the study presented in paper IV was to investigate the effect of (i) the concentration entering intestine, and (ii) the total dose administered, on the first-pass intestinal glucuronidation of raloxifene. This is considered to have an impact on the design of the *in vivo* release rate of a drug when developing immediate- and modified-release formulations. The raloxifene concentration entering the intestine or the dose administered in the gut did not influence the dose-normalized plasma PK ($AUC_{0\text{-}6h}$ and C_{max}) of raloxifene

in the 30-60 mg dose range (Figur 17). The dose-proportionality indicated that the absorption rate of raloxifene followed a first-order kinetic in the investigated dose range. It can be concluded that intestinal glucuronidation of raloxifene in pigs had a high capacity and could not be affected by clinical relevant doses.

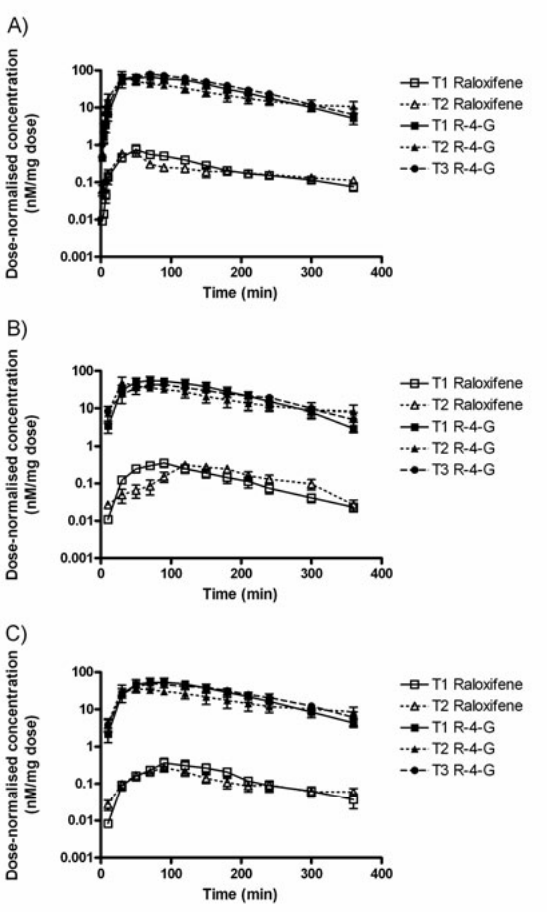

Figure 17. Dose-normalized mean plasma concentrations ± S.E. of raloxifene and the metabolite R-4-G in the three parallel i.j. treatment groups (T1-T3). A) VP B) VH and C) VF.

The pig as an experimental animal

The studies included in this thesis use the pig as an experimental animal. For interspecies comparisons and predictions it is important to characterize the expression, activity and function of membrane and enzymatic proteins in pigs, particularly at a mechanistic level. This will increase the confidence of

extrapolations of observations between pig and human. In Paper II, the *in vitro* metabolism of the human CYP3A4, CYP2C9 and CYP2D6 substrates testosterone, diclofenac and dextromethorphan was determined in pigs (of the same type used in the *in vivo* studies) and directly compared to corresponding human measurements.

The results showed that the metabolic processes of pig and humans have quantitative and qualitative similarities and dissimilarities (Table 7). The CYP3A enzyme system seems to have similar activities in pigs and humans. However, there may be qualitative differences, as the classical CYP3A4 substrate testosterone showed different metabolite patterns in pigs compared to humans (androstenedione was the major metabolite formed in pig liver microsomes in contrast to 6β-OH-testosterone in humans). Therefore, care should always be taken when extrapolating metabolic processes for a new compound between pigs and humans.

Table 7.*Enzyme kinetic parameters of testosterone (TST), dextromethorphan (DXM) and diclofenac (DIC) measured in pig (PLM) and human liver microsomes (HLM).*

Substrates	**Species**	**fu_P**	**V_{max} (pmol/min/mg)**	**K_m (µM)**	**CL_{int} (µl/min/mg)**
Formation of:					
6β-OH-TST	PLM	0.95±0.03	1563±146	262±40	6.0±3.7
	HLM	0.91±0.01	3561±1976	482±337	7.4±5.9
AED	PLM	0.95±0.03	526±12	6.0±1.0	88±12
	HLM	0.91±0.01	81±3.0	15±2.2	5.4±1.4
Depletion of:					
DXM	PLM	0.63±0.23	3263±507	1.9±1.1	1760±810
	HLM	0.72±0.08	1199±217*	11±4.9	110±82
TST	PLM	0.95±0.03	4746±322	45±11	106±20
	HLM	0.91±0.01	1037±1079*	43±53	24±7.0*
DIC	PLM	0.60±0.17	99.1±114	31±43	3.2±1.1
	HLM	0.81±0.06	1159±148**	8.9±1.3	130±5.0***

Values are presented as mean ± SD.
*·**·***Significantly different from pigs (*p<0.05, **p<0.01, ***p<0.001)

The *in vitro* metabolism of the human CYP2C9 substrate diclofenac was very low in pigs and did not correlate to corresponding activity in humans. In contrast dextromethorphan exhibited a very extensive and rapid metabolism in pig liver microsomes compared to those from humans. This data, together with the frequently reported high metabolic activity of known CYP2D6 substrates and high gene expression, indicates that CYP2D is an important CYP subfamily in pigs.

Important enzymes and transporters previously known to be expressed in humans were shown to also exist in pigs (Figure 18). CYP3A expression was the highest of all tested genes in both the intestine and liver, which indicates that pigs have the potential of a high metabolic activity comparable to human CYP3A4. When comparing the levels of expression between the intes-

tine and liver, it was obvious that CYP3A is expressed more abundantly in the liver, while the opposite was true for CYP2C42, ABCB1 and ABCG2. The mRNA data increased the insight into the inter-individual variability and the relative expression of different enzymes and transporters in pig intestine and liver.

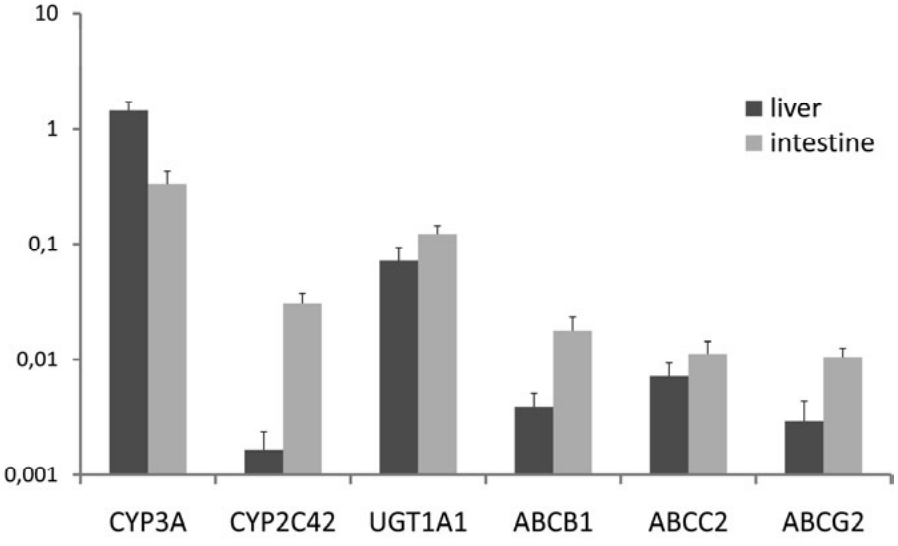

*Figure 18.*The mRNA expression of CYP3A, CYP2C42, UGT1A1, ABCB1, ABCC2 and ABCG2 in pig liver and jejunum when normalized to the expression of villin.

Conclusions

An efficient and successful drug development process relies in detailed knowledge of processes determining the oral F of a drug. This project has pointed out the importance of E_G in the overall first-pass extraction of R/S-VER(CYP3A compound) and raloxifene (UGT compound). This study suggests that E_G should be considered and evaluated early in drug development, e.g. by incorporating this parameter into *in vitro-in vivo* oral CL predictions. The complexity of oral absorption and first-pass extraction of a drug emphasizes the need for an *in vivo* model that enables determination of detailed PK data and the use of a PBPK model to discriminate between processes that determine the PK.

From the investigations presented in this thesis, the major conclusions drawn were:

- The results from the two *in vivo* studies show the usefulness of the multisampling site pig model, with plasma sampling pre and post liver, to identify organ-specific metabolic processes.

- R/S-VER was extensively metabolized in pigs, and the gut mucosa and the liver contributed to this extraction to the same extent. As in humans, the concentration of the S-isomer was lower in plasma than the R-isomer and the stereoselectivity was more pronounced after oral compared to i.v. dosing. The $AUC_{0\text{-}6h}$ R/S ratio was most pronounced in the VH, which indicated that the liver was mainly responsible for the stereoselectivity.

- From the *in vitro* studies it was concluded that the lower plasma concentration of S-VER *in vivo* was probably not due to different CL_{int} for R- and S-VER. The PBPK model could be used to determine that the stereoselective PK of R/S-VER was instead due to a combination of several processes, including enantioselective plasma protein binding, blood-to-plasma partition, and gut and liver tissue distribution. The first-pass effect in the gut and liver after i.j. administration amplified the difference in isomer concentration and explains the absence of stereoselectivity after an i.v. dose.

- Ketoconazole increased the $AUC_{0\text{-}6h}$ and C_{max} of R/S-VER in the VP as a result of inhibition of CYP3A-mediated E_G. However, E_H was increased because the effect of inhibited E_G was not observed at the peripheral plasma sampling sites. A temporary increase in fu_P may explain this unexpected observation.

- In pigs, intestinal glucuronidation has a greater impact on the oral F of raloxifene than hepatic glucuronidation. The raloxifene concentration entering the intestine or the dose administered in the gut did not influence the systemic exposure of the drug; i.e. the gut wall extraction was not saturable with clinical relevant doses.

- A time-dependent E_H was observed for R/S-VER and raloxifene. A report of a constant, single E_H value might be a simplified way of describing the liver extraction of drugs during the absorption phase. This is important to consider when attempting to correlate *in vitro*- and *in vivo* drug absorption.

- Characterization of the *in vitro* metabolism of four model drugs in pig liver microsomes showed that CYP3A4 activity is relatively similar between the two species. A relationship between pig CYP3A mRNA liver expression and *in vivo* E_H of R/S-VER was established.

Populärvetenskaplig sammanfattning

Begreppen biotillgänglighet och första-passage metabolism av läkemedel är av central betydelse för denna avhandling (Figur 19). Det absolut vanligaste sättet att ta ett läkemedel är att svälja en tablett som innehåller en bestämd dos eller mängd av läkemedlet. Allting vi äter och tar upp i kroppen passerar tarmen och levern och nedbrytning av läkemedel kan ske på dessa platser. Det är denna nedbrytning som kallas för första-passage metabolism. Biotillgänglighet är ett begrepp för att beskriva hur mycket som finns kvar av läkemedlet när det når sitt mål. Det är viktigt att studera detta eftersom det är mängden läkemedel som avgör såväl effekt som biverkningar av läkemedlet.

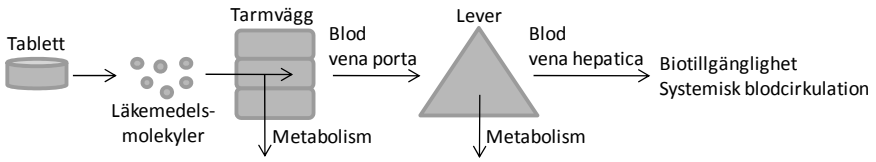

Figure 19. Ett läkemedels väg från att man sväljer ned tabletten till dess att läkemedelsmolekylerna kommer ut i det systemiska blodkretsloppet och kan ge effekt.

Syftet med denna avhandling var att undersöka tarmens betydelse i jämförelse med levern under första-passage metabolism av läkemedel. Främst två olika enzymer har studerats genom användningen av två olika modellsubstanser: R/S-verapamil raloxifen. R/S-verapamil och raloxifen gavs som en lösning i tarmen eller i blodet på levande grisar. Blodprov togs från tre olika vener under 360 min och koncentrationen av läkemedlet bestämdes. Genom att följa läkemedelskoncentrationen över tid i blodet kan man se vad som händer med läkemedlet i kroppen och räkna ut exempelvis hur mycket som metaboliseras i tarmen och levern och hur stor biotillgängligheten av läkemedlet är. I dessa studier kom vi fram till att tarmen har en stor förmåga att metabolisera R/S-verapamil och raloxifen efter oral administrering. R/S-verapamil är en blandning av 50% R- och 50% S-verapamil. Liksom i människor visade det sig att S-formen återfanns i lägre koncentration än R-formen i blodet hos grisar. Detta har betydelse eftersom det är framförallt S-formen som har farmakologisk verkan.

Förutom de två studierna i grisar så gjordes också en jämförelse av hur R/S-verapamil och tre andra läkemedel metaboliseras i levern hos grisar och människor. I denna studie användes en framrening av enzymer som finns

inuti kroppens celler. Med avseende på det enzym som är inblandat i metabolism av mer än 50% av de läkemedel som finns på marknaden idag så visade resultaten att detta enzym har liknande aktivitet i gris och människor. Däremot verkar aktiviteten av två andra enzym vara motsatt i gris och människor. För att kunna överföra resultat från djurstudier till hur det skulle se ut hos människor är det viktigt att ha kunskap om likheter och skillnader mellan arterna.

I ytterligare ett arbete gjordes en fysiologiskt baserad datamodell med organ och blodflöden liknande grisens kroppsuppbyggnad. En sådan typ av modell har blivit allt vanligare att använda inom läkemedelsindustrin för att optimera, påskynda och på så sätt minska kostnaderna vid framställning av ett nytt läkemedel. I arbete III i avhandlingen användes datamodellen till en mer detaljerad och utforskande undersökning av den data som erhölls i arbete I med syfte att hitta anledningen till att R- och S-verapamil finns i olika koncentration i blodet hos grisar. Med modellen som verktyg kunde vi visa att R- och S-verapamil binder olika till komponenter i blodet, tarmen och levern. En annan intressant observation var att metabolism i levern inte var konstant under den 360 min långa tidsperiod då blod samlades från grisarna. Denna observation var kopplad till att verapamil tillfälligt fastnade i levern och att metabolismen hämmades med tiden.

Sammanfattningsvis så har denna avhandling bidragit med detaljerad kunskap om första-passage metabolism av läkemedel och har påvisat att tarmen har stor betydelse i denna process. Vi föreslår att metabolism i tarmen ska undersökas och utvärderas tidigt i läkemedelsframställning, exempelvis genom att inkludera denna parameter i prediktioner med hjälp av datamodeller.

Acknowledgements

The work presented in this thesis was carried out at the Department of Pharmacy, Faculty of Pharmacy, Uppsala University, Sweden. The studies were sponsored by AstraZeneca R&D Alderley Park, Macclesfield, UK.

I would like to express my sincere gratitude for all of you who made this work possible:

Min handledare, professor **Hans Lennernäs**, för din smittsamma energi! Ditt ledarskap med lösa tyglar har varit lärorikt och utvecklande. Jag kommer att sakna dina galna historier och anekdoter. Ett särskilt tack för hjälp och stöd under sista perioden av avhandlingsskrivandet!

Paul Dickinson, my co-supervisor, for providing insight into the pharmaceutical industry and for helpful and wise comments and discussions.

Co-writers, **Mikael Hedeland**, **Ulf Bondesson**, **Mohammed Yasin**, **Johannes Schrickx**, for excellent and fruitful collaboration.

Professor Lars Knutson och Anders Nordgren, medarbetare på Ackis. Utan er hade det här aldrig gått! Tack för er kirurgiska skicklighet, ert tålamod under upplärandet på lab, era svar på alla frågor om grisar, anatomi och fysiologi men framförallt för alla skratt och samtal nere på lab!

Elisabeth Börjesson, medarbetare på SVA. Tack för hjälpen med analys av verapamil-proverna!

Professorerna **Martin Malmsten** och **Göran Alderborn**, som i egenskap av prefekter skapat en trevlig och stimulerande arbetsmiljö.

Stipendiefonder, som möjliggjort deltagande vid flertalet konferenser och resor: Uddeholms resestipendium (Värmlands nation), Elisabeth och Alfred Ahlqvists stiftelse (Apotekarsocieteten) och IF´s stiftelse.

My diploma workers, **Karl** and **Isabel**, for nice and fun collaboration!

Kollegorna vid institutionen för farmaci. Särskilt tack till **doktorandkollegorna** genom åren. Den här tiden har varit så rolig och det är tack vare alla er som funnits i min närhet på institutionen, konferensresor, disputationsfester, doktoranddagar m.m. Vill också passa på att tacka **innebandygänget** för svettiga och trevliga onsdagskvällar!

Alla forna och nuvarande **doktorander i biofarmacigruppen**. Särskilt vill jag tacka: **Anna**, vad skulle den här tiden ha varit utan dig! Tack för allt stöd, allt påhejande, alla lärorika diskussioner och alla roliga stunder på institutionen och ute i världen. **Erik**, min mentor från första stund ända in i mål! Du är med ditt omväxlande och pratglada humör en ovärderlig person att ha som kollega och vän! **Elin**, för kloka och genomtänkta svar, för inspiration till att vilja lära mig mer och för allt roligt vi haft under dessa år! **Ebba**, för din energiska, pratglada och sociala personlighet som medfört många skratt och underhållande stunder!

Familjerna **Fellbrant**, **Hulterström**, **Norberg**, **Mellwing** och **Egeblad/Wellin, Thorell/Persson**, vuxna som barn, samt **Niina** och **"Hemtjänsttjejerna"** för att ni förgyller min fritid med prat, skratt och diverse aktiviteter. Ni betyder alla väldigt mycket för mig!

Familjen Thörn. Framförallt vill jag tacka mina svärföräldrar **Eva** och **Leif** för att ni bryr er om oss så mycket och att ni är världens bästa farmor och farfar till Embla och Vilgot!

Min **mamma** som alltid ställt upp med allt jag bett om och lite till. Utan din hjälp med barnpassning hade det varit svårt att få klart den här boken. **Pappa**, nu är jag faktiskt klar med skolan ☺! Det är du som har lärt mig att hårt arbete lönar sig och att det är upp till en själv att få saker och ting gjorda. Det räckte så långt som till en doktorsavhandling minsann! Mina kära systrar **Madeleine** och **Emelie**, för att ni alltid finns där för mig och för barnen! Ni må vara bäst i sport men nu är jag iaf den mest välutbildade (=klokaste ☺). **Jonas**, min kära svåger, för att du tar så bra hand om både min syster och pappa ☺ och för att det är väldigt roligt att umgås med dig!

Mitt allt, min underbara familj ♥! **Embla** och **Vilgot** för att ni får mig att leva i nuet, för att ni gör mig så glad och för att jag alltid har något att vara stolt över. **Kristofer**, för all tid du "offrat" de sista månaderna, för ovärderlig stöttning i allt jag gör/vill göra och för att du älskar mig för den jag är!

References

1. Pond SM, Tozer TN. First-pass elimination. Basic concepts and clinical consequences. *Clin Pharmacokinet* 1984;9(1):1-25.
2. Wilkinson GR. Drug metabolism and variability among patients in drug response. *N Engl J Med* 2005;352(21):2211-21.
3. Ito K, Iwatsubo T, Kanamitsu S, Ueda K, Suzuki H, Sugiyama Y. Prediction of pharmacokinetic alterations caused by drug-drug interactions: metabolic interaction in the liver. *Pharmacol Rev* 1998;50(3):387-412.
4. CPMP/EWP/560/95/Rev.1. Guidline on the Investigation of Drug Interactions. *European Medicines Agency, London* 2010.
5. Lin JH, Chiba M, Baillie TA. Is the role of the small intestine in first-pass metabolism overemphasized? *Pharmacol Rev* 1999;51(2):135-58.
6. Shen DD, Kunze KL, Thummel KE. Enzyme-catalyzed processes of first-pass hepatic and intestinal drug extraction. *Adv Drug Deliv Rev* 1997;27(2-3):99-127.
7. Doherty MM, Pang KS. First-pass effect: significance of the intestine for absorption and metabolism. *Drug Chem Toxicol* 1997;20(4):329-44.
8. Kato M. Intestinal first-pass metabolism of CYP3A4 substrates. *Drug Metab Pharmacokinet* 2008;23(2):87-94.
9. Agoram B, Woltosz WS, Bolger MB. Predicting the impact of physiological and biochemical processes on oral drug bioavailability. *Adv Drug Deliv Rev* 2001;50 Suppl 1:S41-67.
10. Jamei M, Turner D, Yang J, Neuhoff S, Polak S, Rostami-Hodjegan A, et al. Population-based mechanistic prediction of oral drug absorption. *AAPS J* 2009;11(2):225-37.
11. Madara JLaT, J. S. The functional morphology of the mucosa of the small intestine. In: Johnson LR, editor. *Physiology of the gastrointestinal tract*. New York: Ed. Raven Press 1994:1577-622.
12. Lacy ER. Functional morphology of the large intestine. In: Rauner RB, editor. *Handbook of Physiology 6: The gastrointestinal system*. New York: Oxford University Press, 1997:121-94.
13. Johnson LR. *Gastrointestinal physiology*. St. Louis, MO: Mosby-Year Book, 1997.
14. van Meer G, Simons K. The function of tight junctions in maintaining differences in lipid composition between the apical and the basolateral cell surface domains of MDCK cells. *EMBO J* 1986;5(7):1455-64.

15. Ballard ST, Hunter JH, Taylor AE. Regulation of tight-junction permeability during nutrient absorption across the intestinal epithelium. *Annu Rev Nutr* 1995;15:35-55.
16. Lennernas H. Intestinal permeability and its relevance for absorption and elimination. *Xenobiotica* 2007;37(10-11):1015-51.
17. Sugano K, Kansy M, Artursson P, Avdeef A, Bendels S, Di L, et al. Coexistence of passive and carrier-mediated processes in drug transport. *Nat Rev Drug Discov* 2010;9(8):597-614.
18. Bergstrom CA. Computational models to predict aqueous drug solubility, permeability and intestinal absorption. *Expert Opin Drug Metab Toxicol* 2005;1(4):613-27.
19. Lennernas H. Does fluid flow across the intestinal mucosa affect quantitative oral drug absorption? Is it time for a reevaluation? *Pharm Res* 1995;12(11):1573-82.
20. Giacomini KM, Huang SM, Tweedie DJ, Benet LZ, Brouwer KL, Chu X, et al. Membrane transporters in drug development. *Nat Rev Drug Discov* 2010;9(3):215-36.
21. Lown KS, Mayo RR, Leichtman AB, Hsiao HL, Turgeon DK, Schmiedlin-Ren P, et al. Role of intestinal P-glycoprotein (mdr1) in interpatient variation in the oral bioavailability of cyclosporine. *Clin Pharmacol Ther* 1997;62(3):248-60.
22. Johne A, Kopke K, Gerloff T, Mai I, Rietbrock S, Meisel C, et al. Modulation of steady-state kinetics of digoxin by haplotypes of the P-glycoprotein MDR1 gene. *Clin Pharmacol Ther* 2002;72(5):584-94.
23. Sparreboom A, van Asperen J, Mayer U, Schinkel AH, Smit JW, Meijer DK, et al. Limited oral bioavailability and active epithelial excretion of paclitaxel (Taxol) caused by P-glycoprotein in the intestine. *Proc Natl Acad Sci U S A* 1997;94(5):2031-5.
24. Kim RB, Fromm MF, Wandel C, Leake B, Wood AJ, Roden DM, et al. The drug transporter P-glycoprotein limits oral absorption and brain entry of HIV-1 protease inhibitors. *J Clin Invest* 1998;101(2):289-94.
25. Liu YT, Hao HP, Liu CX, Wang GJ, Xie HG. Drugs as CYP3A probes, inducers, and inhibitors. *Drug Metab Rev* 2007;39(4):699-721.
26. Ding X, Kaminsky LS. Human extrahepatic cytochromes P450: function in xenobiotic metabolism and tissue-selective chemical toxicity in the respiratory and gastrointestinal tracts. *Annu Rev Pharmacol Toxicol* 2003;43:149-73.
27. Fisher MB, Paine MF, Strelevitz TJ, Wrighton SA. The role of hepatic and extrahepatic UDP-glucuronosyltransferases in human drug metabolism. *Drug Metab Rev* 2001;33(3-4):273-97.
28. Kiang TK, Ensom MH, Chang TK. UDP-glucuronosyltransferases and clinical drug-drug interactions. *Pharmacol Ther* 2005;106(1):97-132.
29. Miners JO, Smith PA, Sorich MJ, McKinnon RA, Mackenzie PI. Predicting human drug glucuronidation parameters: application of in vitro and in silico modeling approaches. *Annu Rev Pharmacol Toxicol* 2004;44:1-25.

30. Pacifici GM, Franchi M, Bencini C, Repetti F, Di Lascio N, Muraro GB. Tissue distribution of drug-metabolizing enzymes in humans. *Xenobiotica* 1988;18(7):849-56.
31. Krishna DR, Klotz U. Extrahepatic metabolism of drugs in humans. *Clin Pharmacokinet* 1994;26(2):144-60.
32. Radominska-Pandya A, Little JM, Pandya JT, Tephly TR, King CD, Barone GW, et al. UDP-glucuronosyltransferases in human intestinal mucosa. *Biochim Biophys Acta* 1998;1394(2-3):199-208.
33. Paine MF, Hart HL, Ludington SS, Haining RL, Rettie AE, Zeldin DC. The human intestinal cytochrome P450 "pie". *Drug Metab Dispos* 2006;34(5):880-6.
34. de Waziers I, Cugnenc PH, Yang CS, Leroux JP, Beaune PH. Cytochrome P 450 isoenzymes, epoxide hydrolase and glutathione transferases in rat and human hepatic and extrahepatic tissues. *J Pharmacol Exp Ther* 1990;253(1):387-94.
35. Paine MF, Khalighi M, Fisher JM, Shen DD, Kunze KL, Marsh CL, et al. Characterization of interintestinal and intraintestinal variations in human CYP3A-dependent metabolism. *J Pharmacol Exp Ther* 1997;283(3):1552-62.
36. Yang J, Tucker GT, Rostami-Hodjegan A. Cytochrome P450 3A expression and activity in the human small intestine. *Clin Pharmacol Ther* 2004;76(4):391.
37. Zhang QY, Dunbar D, Ostrowska A, Zeisloft S, Yang J, Kaminsky LS. Characterization of human small intestinal cytochromes P-450. *Drug Metab Dispos* 1999;27(7):804-9.
38. Murray GI, Barnes TS, Sewell HF, Ewen SW, Melvin WT, Burke MD. The immunocytochemical localisation and distribution of cytochrome P-450 in normal human hepatic and extrahepatic tissues with a monoclonal antibody to human cytochrome P-450. *Br J Clin Pharmacol* 1988;25(4):465-75.
39. Tukey RH, Strassburg CP. Human UDP-glucuronosyltransferases: metabolism, expression, and disease. *Annu Rev Pharmacol Toxicol* 2000;40:581-616.
40. Diczfalusy E, Franksson C, Lisboa BP, Martinsen B. Formation of oestrone glucosiduronate by the human intestinal tract. *Acta Endocrinol (Copenh)* 1962;40:537-51.
41. Back DJ, Bates M, Breckenridge AM, Ellis A, Hall JM, Maciver M, et al. The in vitro metabolism of ethinyloestradiol, mestranol and levonorgestrel by human jejunal mucosa. *Br J Clin Pharmacol* 1981;11(3):275-8.
42. Rogers SM, Back DJ, Orme ML. Intestinal metabolism of ethinyloestradiol and paracetamol in vitro: studies using Ussing chambers. *Br J Clin Pharmacol* 1987;23(6):727-34.
43. Peters WH, Kock L, Nagengast FM, Kremers PG. Biotransformation enzymes in human intestine: critical low levels in the colon? *Gut* 1991;32(4):408-12.

44. Pacifici GM, Bencini C, Rane A. Presystemic glucuronidation of morphine in humans and rhesus monkeys: subcellular distribution of the UDP-glucuronyltransferase in the liver and intestine. *Xenobiotica* 1986;16(2):123-8.
45. Cappiello M, Giuliani L, Pacifici GM. Distribution of UDP-glucuronosyltransferase and its endogenous substrate uridine 5'-diphosphoglucuronic acid in human tissues. *Eur J Clin Pharmacol* 1991;41(4):345-50.
46. Cubitt HE, Houston JB, Galetin A. Relative importance of intestinal and hepatic glucuronidation-impact on the prediction of drug clearance. *Pharm Res* 2009;26(5):1073-83.
47. Bernard O, Guillemette C. The main role of UGT1A9 in the hepatic metabolism of mycophenolic acid and the effects of naturally occurring variants. *Drug Metab Dispos* 2004;32(8):775-8.
48. Bowalgaha K, Miners JO. The glucuronidation of mycophenolic acid by human liver, kidney and jejunum microsomes. *Br J Clin Pharmacol* 2001;52(5):605-9.
49. Watanabe Y, Nakajima M, Yokoi T. Troglitazone glucuronidation in human liver and intestine microsomes: high catalytic activity of UGT1A8 and UGT1A10. *Drug Metab Dispos* 2002;30(12):1462-9.
50. Kolars JC, Awni WM, Merion RM, Watkins PB. First-pass metabolism of cyclosporin by the gut. *Lancet* 1991;338(8781):1488-90.
51. Paine MF, Shen DD, Kunze KL, Perkins JD, Marsh CL, McVicar JP, et al. First-pass metabolism of midazolam by the human intestine. *Clin Pharmacol Ther* 1996;60(1):14-24.
52. Sandstrom R, Karlsson A, Knutson L, Lennernas H. Jejunal absorption and metabolism of R/S-verapamil in humans. *Pharm Res* 1998;15(6):856-62.
53. von Richter O, Greiner B, Fromm MF, Fraser R, Omari T, Barclay ML, et al. Determination of in vivo absorption, metabolism, and transport of drugs by the human intestinal wall and liver with a novel perfusion technique. *Clin Pharmacol Ther* 2001;70(3):217-27.
54. Fromm MF, Busse D, Kroemer HK, Eichelbaum M. Differential induction of prehepatic and hepatic metabolism of verapamil by rifampin. *Hepatology* 1996;24(4):796-801.
55. Hebert MF, Roberts JP, Prueksaritanont T, Benet LZ. Bioavailability of cyclosporine with concomitant rifampin administration is markedly less than predicted by hepatic enzyme induction. *Clin Pharmacol Ther* 1992;52(5):453-7.
56. Wu CY, Benet LZ, Hebert MF, Gupta SK, Rowland M, Gomez DY, et al. Differentiation of absorption and first-pass gut and hepatic metabolism in humans: studies with cyclosporine. *Clin Pharmacol Ther* 1995;58(5):492-7.
57. Holtbecker N, Fromm MF, Kroemer HK, Ohnhaus EE, Heidemann H. The nifedipine-rifampin interaction. Evidence for induction of gut wall metabolism. *Drug Metab Dispos* 1996;24(10):1121-3.

58. Thummel KE, O'Shea D, Paine MF, Shen DD, Kunze KL, Perkins JD, et al. Oral first-pass elimination of midazolam involves both gastrointestinal and hepatic CYP3A-mediated metabolism. *Clin Pharmacol Ther* 1996;59(5):491-502.
59. Regardh CG, Edgar B, Olsson R, Kendall M, Collste P, Shansky C. Pharmacokinetics of felodipine in patients with liver disease. *Eur J Clin Pharmacol* 1989;36(5):473-9.
60. Sandstrom R, Knutson TW, Knutson L, Jansson B, Lennernas H. The effect of ketoconazole on the jejunal permeability and CYP3A metabolism of (R/S)-verapamil in humans. *Br J Clin Pharmacol* 1999;48(2):180-9.
61. Seidegard J, Nyberg L, Borga O. Presystemic elimination of budesonide in man when administered locally at different levels in the gut, with and without local inhibition by ketoconazole. *Eur J Pharm Sci* 2008;35(4):264-70.
62. Skottheim IB, Jakobsen GS, Stormark K, Christensen H, Hjelmesaeth J, Jenssen T, et al. Significant increase in systemic exposure of atorvastatin after biliopancreatic diversion with duodenal switch. *Clin Pharmacol Ther* 2010;87(6):699-705.
63. Veroli P, O'Kelly B, Bertrand F, Trouvin JH, Farinotti R, Ecoffey C. Extrahepatic metabolism of propofol in man during the anhepatic phase of orthotopic liver transplantation. *Br J Anaesth* 1992;68(2):183-6.
64. Raoof AA, van Obbergh LJ, de Ville de Goyet J, Verbeeck RK. Extrahepatic glucuronidation of propofol in man: possible contribution of gut wall and kidney. *Eur J Clin Pharmacol* 1996;50(1-2):91-6.
65. Cassidy MK, Houston JB. In vivo assessment of extrahepatic conjugative metabolism in first pass effects using the model compound phenol. *J Pharm Pharmacol* 1980;32(1):57-9.
66. Cassidy MK, Houston JB. In vivo capacity of hepatic and extrahepatic enzymes to conjugate phenol. *Drug Metab Dispos* 1984;12(5):619-24.
67. Mistry M, Houston JB. Quantitation of extrahepatic metabolism. Pulmonary and intestinal conjugation of naphthol. *Drug Metab Dispos* 1985;13(6):740-5.
68. Mistry M, Houston JB. Glucuronidation in vitro and in vivo. Comparison of intestinal and hepatic conjugation of morphine, naloxone, and buprenorphine. *Drug Metab Dispos* 1987;15(5):710-7.
69. Benet LZ, Cummins CL. The drug efflux-metabolism alliance: biochemical aspects. *Adv Drug Deliv Rev* 2001;50 Suppl 1:S3-11.
70. Watkins PB. The barrier function of CYP3A4 and P-glycoprotein in the small bowel. *Adv Drug Deliv Rev* 1997;27(2-3):161-70.
71. Benet LZ. The drug transporter-metabolism alliance: uncovering and defining the interplay. *Mol Pharm* 2009;6(6):1631-43.
72. Webborn PJ, Parker AJ, Denton RL, Riley RJ. In vitro-in vivo extrapolation of hepatic clearance involving active uptake: theoretical and experimental aspects. *Xenobiotica* 2007;37(10-11):1090-109.

73. Baker M, Parton T. Kinetic determinants of hepatic clearance: plasma protein binding and hepatic uptake. *Xenobiotica* 2007;37(10-11):1110-34.
74. Roberts MS, Magnusson BM, Burczynski FJ, Weiss M. Enterohepatic circulation: physiological, pharmacokinetic and clinical implications. *Clin Pharmacokinet* 2002;41(10):751-90.
75. Desmet VJ. Organizational principles. *The liver biology and pathobiology*. 4 ed, 2001:3-17.
76. Evans WH. A biochemical dissection of the functional polarity of the plasma membrane of the hepatocyte. *Biochim Biophys Acta* 1980;604(1):27-64.
77. Dean M, Hamon Y, Chimini G. The human ATP-binding cassette (ABC) transporter superfamily. *J Lipid Res* 2001;42(7):1007-17.
78. Hediger MA, Romero MF, Peng JB, Rolfs A, Takanaga H, Bruford EA. The ABCs of solute carriers: physiological, pathological and therapeutic implications of human membrane transport proteinsIntroduction. *Pflugers Arch* 2004;447(5):465-8.
79. Borst P, Elferink RO. Mammalian ABC transporters in health and disease. *Annu Rev Biochem* 2002;71:537-92.
80. Rendic S. Summary of information on human CYP enzymes: human P450 metabolism data. *Drug Metab Rev* 2002;34(1-2):83-448.
81. Zamek-Gliszczynski MJ, Hoffmaster KA, Nezasa K, Tallman MN, Brouwer KL. Integration of hepatic drug transporters and phase II metabolizing enzymes: mechanisms of hepatic excretion of sulfate, glucuronide, and glutathione metabolites. *Eur J Pharm Sci* 2006;27(5):447-86.
82. Shimada T, Yamazaki H, Mimura M, Inui Y, Guengerich FP. Interindividual variations in human liver cytochrome P-450 enzymes involved in the oxidation of drugs, carcinogens and toxic chemicals: studies with liver microsomes of 30 Japanese and 30 Caucasians. *J Pharmacol Exp Ther* 1994;270(1):414-23.
83. Luo G, Johnson S, Hsueh MM, Zheng J, Cai H, Xin B, et al. In silico prediction of biliary excretion of drugs in rats based on physicochemical properties. *Drug Metab Dispos* 2010;38(3):422-30.
84. Rowland M, Peck C, Tucker G. Physiologically-based pharmacokinetics in drug development and regulatory science. *Annu Rev Pharmacol Toxicol* 2011;51:45-73.
85. Poulin P, Jones RD, Jones HM, Gibson CR, Rowland M, Chien JY, et al. PHRMA CPCDC initiative on predictive models of human pharmacokinetics, part 5: Prediction of plasma concentration-time profiles in human by using the physiologically-based pharmacokinetic modeling approach. *J Pharm Sci* 2011.
86. Ito K, Houston JB. Prediction of human drug clearance from in vitro and preclinical data using physiologically based and empirical approaches. *Pharm Res* 2005;22(1):103-12.

87. Rostami-Hodjegan A, Tucker GT. Simulation and prediction of in vivo drug metabolism in human populations from in vitro data. *Nat Rev Drug Discov* 2007;6(2):140-8.
88. Lave T, Coassolo P, Reigner B. Prediction of hepatic metabolic clearance based on interspecies allometric scaling techniques and in vitro-in vivo correlations. *Clin Pharmacokinet* 1999;36(3):211-31.
89. Gertz M, Houston JB, Galetin A. Physiologically based pharmacokinetic modeling of intestinal first-pass metabolism of CYP3A substrates with high intestinal extraction. *Drug Metab Dispos* 2011;39(9):1633-42.
90. Yang J, Jamei M, Yeo KR, Tucker GT, Rostami-Hodjegan A. Prediction of intestinal first-pass drug metabolism. *Curr Drug Metab* 2007;8(7):676-84.
91. Galetin A. Intestinal first-pass metabolism: bridging the gap between in vitro and in vivo. *Curr Drug Metab* 2007;8(7):643-4.
92. Kadono K, Akabane T, Tabata K, Gato K, Terashita S, Teramura T. Quantitative prediction of intestinal metabolism in humans from a simplified intestinal availability model and empirical scaling factor. *Drug Metab Dispos* 2010;38(7):1230-7.
93. Galetin A, Houston JB. Intestinal and hepatic metabolic activity of five cytochrome P450 enzymes: impact on prediction of first-pass metabolism. *J Pharmacol Exp Ther* 2006;318(3):1220-9.
94. Lave T, Chapman K, Goldsmith P, Rowland M. Human clearance prediction: shifting the paradigm. *Expert Opin Drug Metab Toxicol* 2009;5(9):1039-48.
95. Jones HM, Parrott N, Jorga K, Lave T. A novel strategy for physiologically based predictions of human pharmacokinetics. *Clin Pharmacokinet* 2006;45(5):511-42.
96. Houston JB, Galetin A. Methods for predicting in vivo pharmacokinetics using data from in vitro assays. *Curr Drug Metab* 2008;9(9):940-51.
97. Pelkonen O, Turpeinen M. In vitro-in vivo extrapolation of hepatic clearance: biological tools, scaling factors, model assumptions and correct concentrations. *Xenobiotica* 2007;37(10-11):1066-89.
98. Lave T, Parrott N, Grimm HP, Fleury A, Reddy M. Challenges and opportunities with modelling and simulation in drug discovery and drug development. *Xenobiotica* 2007;37(10-11):1295-310.
99. Badhan R, Penny J, Galetin A, Houston JB. Methodology for development of a physiological model incorporating CYP3A and P-glycoprotein for the prediction of intestinal drug absorption. *J Pharm Sci* 2009;98(6):2180-97.
100. Fenneteau F, Poulin P, Nekka F. Physiologically based predictions of the impact of inhibition of intestinal and hepatic metabolism on human pharmacokinetics of CYP3A substrates. *J Pharm Sci* 2010;99(1):486-514.
101. Darwich AS, Neuhoff S, Jamei M, Rostami-Hodjegan A. Interplay of metabolism and transport in determining oral drug absorption and gut

wall metabolism: a simulation assessment using the "advanced dissolution, absorption, metabolism (ADAM)" model. *Curr Drug Metab* 2010;11(9):716-29.
102. Eichelbaum M, Ende M, Remberg G, Schomerus M, Dengler HJ. The metabolism of DL-[14C]verapamil in man. *Drug Metab Dispos* 1978;7(3):145-8.
103. Hamann SR, Blouin RA, McAllister RG, Jr. Clinical pharmacokinetics of verapamil. *Clin Pharmacokinet* 1984;9(1):26-41.
104. Winiwarter S, Bonham NM, Ax F, Hallberg A, Lennernas H, Karlen A. Correlation of human jejunal permeability (in vivo) of drugs with experimentally and theoretically derived parameters. A multivariate data analysis approach. *J Med Chem* 1998;41(25):4939-49.
105. Benet LZ, Amidon GL, Barends DM, Lennernas H, Polli JE, Shah VP, et al. The use of BDDCS in classifying the permeability of marketed drugs. *Pharm Res* 2008;25(3):483-8.
106. Custodio JM, Wu CY, Benet LZ. Predicting drug disposition, absorption/elimination/transporter interplay and the role of food on drug absorption. *Adv Drug Deliv Rev* 2008;60(6):717-33.
107. Amidon GL, Lennernas H, Shah VP, Crison JR. A theoretical basis for a biopharmaceutic drug classification: the correlation of in vitro drug product dissolution and in vivo bioavailability. *Pharm Res* 1995;12(3):413-20.
108. Vogelgesang B, Echizen H, Schmidt E, Eichelbaum M. Stereoselective first-pass metabolism of highly cleared drugs: studies of the bioavailability of L- and D-verapamil examined with a stable isotope technique. *Br J Clin Pharmacol* 1984;18(5):733-40.
109. Petri N, Bergman E, Forsell P, Hedeland M, Bondesson U, Knutson L, et al. First-pass effects of verapamil on the intestinal absorption and liver disposition of fexofenadine in the porcine model. *Drug Metab Dispos* 2006;34(7):1182-9.
110. Sandstrom R, Lennernas H. Repeated oral rifampicin decreases the jejunal permeability of R/S-verapamil in rats. *Drug Metab Dispos* 1999;27(8):951-5.
111. Kroemer HK, Gautier JC, Beaune P, Henderson C, Wolf CR, Eichelbaum M. Identification of P450 enzymes involved in metabolism of verapamil in humans. *Naunyn Schmiedebergs Arch Pharmacol* 1993;348(3):332-7.
112. Tracy TS, Korzekwa KR, Gonzalez FJ, Wainer IW. Cytochrome P450 isoforms involved in metabolism of the enantiomers of verapamil and norverapamil. *Br J Clin Pharmacol* 1999;47(5):545-52.
113. Benet LZ, Broccatelli F, Oprea TI. BDDCS Applied to Over 900 Drugs. *AAPS J* 2011.
114. Cubitt HE, Houston JB, Galetin A. Prediction of human drug clearance by multiple metabolic pathways: integration of hepatic and intestinal microsomal and cytosolic data. *Drug Metab Dispos* 2011;39(5):864-73.

115. Kemp DC, Fan PW, Stevens JC. Characterization of raloxifene glucuronidation in vitro: contribution of intestinal metabolism to presystemic clearance. *Drug Metab Dispos* 2002;30(6):694-700.
116. Hochner-Celnikier D. Pharmacokinetics of raloxifene and its clinical application. *Eur J Obstet Gynecol Reprod Biol* 1999;85(1):23-9.
117. Jeong EJ, Lin H, Hu M. Disposition mechanisms of raloxifene in the human intestinal Caco-2 model. *J Pharmacol Exp Ther* 2004;310(1):376-85.
118. Chang JH, Kochansky CJ, Shou M. The role of P-glycoprotein in the bioactivation of raloxifene. *Drug Metab Dispos* 2006;34(12):2073-8.
119. Anzenbacher P, Soucek P, Anzenbacherova E, Gut I, Hruby K, Svoboda Z, et al. Presence and activity of cytochrome P450 isoforms in minipig liver microsomes. Comparison with human liver samples. *Drug Metab Dispos* 1998;26(1):56-9.
120. Hannon JP, Bossone CA, Wade CE. Normal physiological values for conscious pigs used in biomedical research. *Lab Anim Sci* 1990;40(3):293-8.
121. Kararli TT. Comparison of the gastrointestinal anatomy, physiology, and biochemistry of humans and commonly used laboratory animals. *Biopharm Drug Dispos* 1995;16(5):351-80.
122. Bogaards JJ, Bertrand M, Jackson P, Oudshoorn MJ, Weaver RJ, van Bladeren PJ, et al. Determining the best animal model for human cytochrome P450 activities: a comparison of mouse, rat, rabbit, dog, micropig, monkey and man. *Xenobiotica* 2000;30(12):1131-52.
123. Nebbia C, Dacasto M, Rossetto Giaccherino A, Giuliano Albo A, Carletti M. Comparative expression of liver cytochrome P450-dependent monooxygenases in the horse and in other agricultural and laboratory species. *Vet J* 2003;165(1):53-64.
124. Skaanild MT, Friis C. Cytochrome P450 sex differences in minipigs and conventional pigs. *Pharmacol Toxicol* 1999;85(4):174-80.
125. Skaanild MT, Friis C. Is cytochrome P450 CYP2D activity present in pig liver? *Pharmacol Toxicol* 2002;91(4):198-203.
126. Assessing abundance of cytochrome P450 enzymes using mass spectrometry based methods: analysis of porcine liver. Drug metabolism Discussion Group Meeting; 2010 September 15-17th; Canterbury, UK.
127. Bergman E, Lundahl A, Fridblom P, Hedeland M, Bondesson U, Knutson L, et al. Enterohepatic disposition of rosuvastatin in pigs and the impact of concomitant dosing with cyclosporine and gemfibrozil. *Drug Metab Dispos* 2009;37(12):2349-58.
128. Persson EM, Nordgren A, Forsell P, Knutson L, Ohgren C, Forssen S, et al. Improved understanding of the effect of food on drug absorption and bioavailability for lipophilic compounds using an intestinal pig perfusion model. *Eur J Pharm Sci* 2008;34(1):22-9.
129. Lundahl A, Hedeland M, Bondesson U, Lennernas H. In vivo investigation in pigs of intestinal absorption, hepatobiliary disposition

and metabolism of the 5-alpha reductase inhibitor finasteride and the effects of co-administered ketoconazole. *Drug Metab Dispos* 2011.
130. Sjodin E, Fritsch H, Eriksson UG, Logren U, Nordgren A, Forsell P, et al. Intestinal and hepatobiliary transport of ximelagatran and its metabolites in pigs. *Drug Metab Dispos* 2008;36(8):1519-28.
131. Bergman E, Hedeland M, Bondesson U, Lennernas H. The effect of acute administration of rifampicin and imatinib on the enterohepatic transport of rosuvastatin in vivo. *Xenobiotica* 2010;40(8):558-68.
132. Sjogren E, Lennernas H, Andersson TB, Grasjo J, Bredberg U. The multiple depletion curves method provides accurate estimates of intrinsic clearance (CLint), maximum velocity of the metabolic reaction (Vmax), and Michaelis constant (Km): accuracy and robustness evaluated through experimental data and Monte Carlo simulations. *Drug Metab Dispos* 2009;37(1):47-58.
133. Vandesompele J, De Preter K, Pattyn F, Poppe B, Van Roy N, De Paepe A, et al. Accurate normalization of real-time quantitative RT-PCR data by geometric averaging of multiple internal control genes. *Genome Biol* 2002;3(7):RESEARCH0034.
134. Elowsson P, Carlsten J. Body composition of the 12-week-old pig studied by dissection. *Lab Anim Sci* 1997;47(2):200-2.
135. Nordgren A, Karlsson T, Wiklund L. Glutamine concentration and tissue exchange with intravenously administered alpha-ketoglutaric acid and ammonium: a dose-response study in the pig. *Nutrition* 2002;18(6):496-504.
136. Poulin P, Theil FP. Prediction of pharmacokinetics prior to in vivo studies. II. Generic physiologically based pharmacokinetic models of drug disposition. *J Pharm Sci* 2002;91(5):1358-70.
137. Matsson EM, Palm JE, Eriksson UG, Bottner P, Lundahl A, Knutson L, et al. Effects of Ketoconazole on the In Vivo Biotransformation and Hepatobiliary Transport of the Thrombin Inhibitor AZD0837 in Pigs. *Drug Metab Dispos* 2011;39(2):239-46.
138. Wang YH, Jones DR, Hall SD. Prediction of cytochrome P450 3A inhibition by verapamil enantiomers and their metabolites. *Drug Metab Dispos* 2004;32(2):259-66.
139. Wang YH, Jones DR, Hall SD. Differential mechanism-based inhibition of CYP3A4 and CYP3A5 by verapamil. *Drug Metab Dispos* 2005;33(5):664-71.
140. Zhou S, Chan E, Lim LY, Boelsterli UA, Li SC, Wang J, et al. Therapeutic drugs that behave as mechanism-based inhibitors of cytochrome P450 3A4. *Curr Drug Metab* 2004;5(5):415-42.
141. Zhou S, Yung Chan S, Cher Goh B, Chan E, Duan W, Huang M, et al. Mechanism-based inhibition of cytochrome P450 3A4 by therapeutic drugs. *Clin Pharmacokinet* 2005;44(3):279-304.

Acta Universitatis Upsaliensis

Digital Comprehensive Summaries of Uppsala Dissertations from the Faculty of Pharmacy 153

Editor: The Dean of the Faculty of Pharmacy

A doctoral dissertation from the Faculty of Pharmacy, Uppsala University, is usually a summary of a number of papers. A few copies of the complete dissertation are kept at major Swedish research libraries, while the summary alone is distributed internationally through the series Digital Comprehensive Summaries of Uppsala Dissertations from the Faculty of Pharmacy.

Distribution: publications.uu.se
urn:nbn:se:uu:diva-165514

ACTA
UNIVERSITATIS
UPSALIENSIS
UPPSALA
2012